

Numerical Analysis of Solar Chimneys for Ventilation in Building

A Thesis Submitted

In partial fulfillment for the reward of the degree of Master of technology

In Mechanical Engineering

SUBMITTED BY

Shivam Singh

(2k19/The/11)

Under the Guidance of

Prof. Anil Kumar

Associate Professor



**Department of Mechanical, Production & Industrial and Automobile
Engineering**

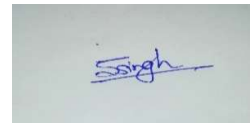
Delhi Technological University

Bawana Road, Delhi-110042

CANDIDATE'S DECLARATION

I, hereby certify that the work which is being presented in thesis entitled “**Numerical Analysis of Solar Chimneys for Ventilation in Building**” being submitted by me is an authentic record of my own work carried out under the supervision of Dr. Anil Kumar, Associate Professor, Department of Mechanical Engineering, Delhi Technological University Delhi.

The matter presented in this thesis has not been submitted in any other University/Institute for the award of M. Tech Degree.

A rectangular box containing a handwritten signature in blue ink that reads "Singh".

SHIVAM SINGH
(2K19/THE/11)

CERTIFICATE

I, hereby rectify that the work which is being presented in this thesis entitled “**Numerical Analysis of Solar Chimneys for Ventilation in Building**” in the partial fulfillment of requirement for the reward of degree of Masters of Technology in Thermal Engineering submitted in the Department of Mechanical Engineering, Delhi Technological University Delhi is an authentic record of my own work carried out during a period from July 2020 to June 2021, under the supervision of Prof. Dr. Anil Kumar, Department of Mechanical Engineering, Delhi Technological University Delhi. The matter presented in this thesis has not been submitted in any other University/Institute for the award of M. Tech Degree.

Dr. Anil Kumar
Supervisor
Department of Mechanical Engineering
Delhi Technological University, Delhi

ACKNOWLEDGEMENT

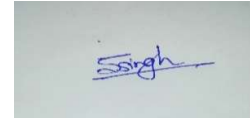
First and foremost, praise and thanks go to my God for the blessing that has bestowed upon me in all my endeavors.

I am profoundly thankful of the inspiration, direction, titillation and patience of Dr. ANIL KUMAR, Associate Professor, my advisor and guide. I appreciate his wide range of experience and attention to detail, as well as his consistent support over the years. It should not be mentioned that a large part of this study is a consequence of collaborative collaboration, without which it would not have been possible to complete the work.

I sincerely thank Prof Dr. ANIL KUMAR for his guidance and relentless support over the year. I am thankful for his worthy suggestions and timely cooperation during his work on the project.

I would like to extend my gratitude to Prof. S. K. Garg, Head, Mechanical Engineering Department for providing this opportunity to carry out this present work.

I would like to thank my family members in this occasion for their moral support and motivation to complete this project in due course.

A rectangular box containing a handwritten signature in blue ink that reads "Singh".

**SHIVAM SINGH
(2K19/THE/11)**

ABSTRACT

The ventilation of buildings is essential to improve the air quality indoors and thermal comfort. Mechanical ventilation systems are now most often used in buildings, such as air conditioning and ventilation. This equipment however consumes a lot of electricity, generated mainly by fossil fuels, which lead to greenhouse gas releases and thus to climate change. As such, it is important to switch to environmentally friendly natural ventilation systems based on renewable energy sources. The solar chimney, which can be mounted or walled up into buildings, is such a natural ventilation system.

This study aimed to develop a mathematical model that evaluates the thermal performance of solar chimneys mounted in inclined or wall mounted. The model has been validated with CFD digital simulations. In order to compare their results with regard to the ventilation rate expresses as the number of air changes per hour, ACH, CFD designed and model various configurations of solar chimneys. For, Jodhpur, India, crude climate information was obtained, including global and diffuse solar radiation intensities on a horizontal plane, wind speed and ambient temperature. This was used in the modelling of solar chimneys by CFD. The effect on the thermal performance of solar chimneys from inclination angle, air gap, and chimney height and view factor was examined in the current study.

The results show good agreement between modelled data from this research and literature-reported experimental values. The root mean square errors were respectively 13 & 20 % for models with and without the view factor. Moreover, a tilting angle of 60° was found to be the optimal tilting angle for as this angle achieved the maximum ventilation rate. Furthermore, the ventilation rate increased, with the air gap increased. When the chimney height was increased, a rise in ACH was observed. It was also noted that when designed to achieve more realistic ventilation rate values, the view factor was an important parameter to be seen. Additionally, ACH has been increased by the inclusion of the view factor. Overall, sloping solar chimneys with a roof give higher thermal performance than

vertical solar chimneys mounted on a wall. Furthermore, the inclusion of the viewing factor increases the precision of the modelling of a solar chimney.

Table of Contents

CHAPTER 1	10
1. INTRODUCTION	10
1.1 Safety of Energy	10
1.2 Ventilation.....	10
1.2.1 Natural ventilation.....	11
1.2.2 The need for natural ventilation	11
1.2.3 Drivers of Natural Ventilation in Buildings.....	12
1.3 Climate change.....	12
1.4 Solar Chimney.....	13
1.4.1 Wall-mounted solar chimney	13
1.4.2 Roof Solar Chimneys	14
1.4.3 Parameters affecting the performance of solar chimneys	15
1.5 Solar Energy's Applications	20
1.6 Absorption of solar radiation as heat.....	20
1.7 Thesis organization	21
CHAPTER 2	23
2. LITERATURE REVIEW	23
2.1 Some Previous Study	23
2.2 Problem Statement	25
2.3 Literature Review of Mathematical modelling	26
2.4 Scope of study	28
2.5 Aim and Objectives.....	29

CHAPTER 3	30
3. METHODOLOGY	30
3.1 The primary energy source for electricity generation	30
3.2 Solar radiation Physics	33
3.2.1 Direct radiation.....	34
3.2.2 Diffuse Radiation	34
3.2.3 Parameters of Geographical & Astronomical	35
3.2.4 Latitude and longitude.....	35
3.2.5 Declination Angles.....	36
3.2.6 Solar Time	36
3.2.7 Hour Angle & Sunset Hour Angle	37
3.2.8 Solar Zenith Angle & Surface Azimuth Angle	37
3.2.9 Incidence angle.....	37
3.2.10 Albedo	38
3.3 Solar radiation modeling on inclined planes	38
3.3.1 Solar constant	38
3.3.2 Extraterrestrial Solar Radiation.....	38
3.3.3 Solar radiation on a tilt surface: beam, diffuse & ground reflected ...	38
3.4 Design of solar chimneys	42
3.4.1 Design parameters of solar chimneys	43
3.5 Mathematical Models.....	46
3.5.1 Assumptions	47
3.5.2 Energy balance equations.....	47
3.5.3 Glass cover with Energy Balance	47

3.5.4	Energy Balance on absorber wall.....	47
3.5.5	Air flow Energy balance	48
3.5.6	Balance of Mass	49
3.6	Solution Procedure	49
3.6.1	Astronomical parameters	49
3.6.2	Attenuation & Radiation of Solar	50
3.6.3	Components of the solar chimney's temperature	52
3.6.4	Correlations of convective heat transfer	53
3.6.5	Coefficients of Heat transfer	55
	CHAPTER 4	58
4.	RESULTS & DISCUSSION.....	58
4.1	Results of Climate data	58
4.2	Simulation in CFD	60
4.2.1	Performance Evaluation of Solar Chimneys	61
4.2.2	Analysis of statistic	62
4.2.3	Solar radiation incident on sloping and vertical surfaces.....	63
4.3	Validation of the Model	64
4.4	System component temperatures.....	65
4.4.1	Temperatures of the glass cover, wall, fluid, & ambient air absorbent	65
4.4.2	Comparison of inclined solar chimney temperatures with vertical solar chimney	68
4.5	The impact of the inclination angle on the ACH	70
4.6	The impact of the air gap on ACH.....	72
4.7	Effect of chimney height on ACH.....	74

4.8	Effect of view factor.....	76
4.8.1	The influence of the view factor on the radiative heat transfer coefficient between the absorber wall and the glass cover	76
4.8.2	View factor going on absorber wall temperatures	77
4.8.3	View factor effect on ACH	79
4.8.4	View factor effect on ACH for various air gap values.....	80
4.8.5	Changes in chimney height have an effect on ACH	82
CHAPTER 5		85
5.	CONCLUSION & RECOMMENDATION	85
5.1	Conclusions	85
5.1.1	Mathematical Model Validation	85
5.1.2	Optimal solar chimney inclination angle	86
5.1.3	Solar chimney Optimum air gap	86
5.1.4	Optimal height of Solar Chimney	86
5.1.5	The main functional view factor in solar chimney design	86
5.2	Recommendations	87
5.2.1	Construction of physical models of solar chimneys placed on roof and wall-mounted	87
5.2.2	Make a comparison with other sites' results.....	87
5.2.3	Investigate the model and the effects of additional factors on solar chimney performance.....	87
5.2.4	Carry out an economic analysis on the feasibility	87
CHAPTER 6		89
6.	REFERENCE.....	89

List of Tables

TABLE 1.1: THE OPTIMAL INCLINATION ANGLE VARIES WITH LATITUDE	19
TABLE 3.1: MODELS OF SOLAR RADIATION	40
TABLE 3.2: OPTIMUM TILT ANGLE FOR SOLAR COLLECTOR.....	44
TABLE 3.3: FOR REFERENCE SITUATIONS, DESIGN PARAMETERS FOR SOLAR CHIMNEY	46
TABLE 3.4: PARAMETER INVESTIGATED IN THIS STUDY	46
TABLE 4.1: COMPARISON OF MATHUR, MATHUR AND ANUPMA EXPERIMENTAL RESULTS FROM 2006 WITH NUMERICAL RESULTS FOR THE INCLINED SOLAR CHIMNEY (45°) DERIVED FROM THE MODEL IN THIS STUDY. THE VIEW FACTOR IS INCLUDED IN MODEL 1 BUT NOT IN MODEL 2.....	64

List of Figures

FIGURE 1.1 WALL SOLAR CHIMNEY DIAGRAM	14
FIGURE 1.2 A ROOFTOP SOLAR CHIMNEY DIAGRAM	15
FIGURE 1.3 A SOLAR CHIMNEY DIAGRAM	21
FIGURE 3.1: IN 2020, THE GLOBAL POWER GENERATED BY EACH ENERGY SOURCE WILL BE CALCULATED, IEA (INTERNATIONAL ENERGY AGENCY) (2020).	31
FIGURE 3.2: IN 2020, RESIDENTIAL (BUILDINGS) AND OTHER SECTORS WILL USE A LARGER PERCENTAGE OF GLOBAL FINAL ENERGY CONSUMPTION. AGRICULTURE AND OTHER UNSPECIFIED SECTORS ARE AMONG THE OTHERS. ADAPTED FROM THE INTERNATIONAL ENERGY AGENCY (2020)	31
FIGURE 3.3: INDIA'S ELECTRICITY GENERATION BY FUEL TYPE IN 2020. ADAPTED FROM IEA (2020).....	32
FIGURE 3.4: INDIA'S FINAL ENERGY USAGE IN THE BUILDING SECTOR. SOURCE: IEA (2020)	33
FIGURE 3.5: BEAM RADIATION ON A SLANTED SURFACE.	34

FIGURE 3.6: DIFFUSE RADIATION ON A TILT SURFACE.	35
FIGURE 3.7: COMPONENTS OF SOLAR RADIATION ON TILT SURFACE.	40
FIGURE 3.8 (A) & (B): SOLAR CHIMNEY MOUNTED ON A WALL.	42
FIGURE 3.9: LOCATION OF JODHPUR INDIA.....	44
FIGURE 4.1: MONTHLY AVERAGE GLOBAL (I_G) & DIFFUSE INSOLATION (I_D) GIVEN IN INDIA ON A HORIZONTAL SURFACE.	59
FIGURE 4.2: MONTHLY AVERAGE AMBIENT AIR TEMPERATURE & WIND SPEED IN JODHPUR INDIA.	60
FIGURE 4.3: AVERAGE MONTHLY INCIDENT INSOLATION ON INCLINED & VERTICAL SURFACES (I_T) IN THE JODHPUR, INDIA.	64
FIGURE 4.4: AVERAGE MONTHLY TEMPERATURES ARE 34° TO $D=0.25$ M AND $L_{ABS}=L_G=2$ M FOR ABSORBER WALL ($T_{W, AVE}$), GLASS COVER ($T_{G, AVE}$), FLUID ($T_{F, AVE}$) AND AMBIENT AIR ($T_{A, AVE}$) FOR THE SOLAR CHIMNEY IN INDIA.	66
FIGURE 4.5: AVERAGE MONTHLY TEMPERATURE IS VERTICAL TO $D=0.25$ M AND $L_{ABS}=L_G=2$ M FOR ABSORBER WALL ($T_{W, AVE}$), GLASS COVER ($T_{G, AVE}$), FLUID ($T_{F, AVE}$) AND AMBIENT AIR ($T_{A, AVE}$) FOR THE SOLAR CHIMNEY IN INDIA.	67
FIGURE 4.6: AVERAGE MONTHLY FLUID ($T_{F, AVE}$) TEMPERATURE FOR TILTED SOLAR PANELS WITH 34° INCLINED ANGLES AND VERTICAL SOLAR PANELS; $D=0.25$ M AND $L_{ABS}=L_G=2$ M IN INDIA.	69
FIGURE 4.7: TEMPERATURES OF AVERAGE MONTHLY GLASS COVERED BY A TILT ANGLE OF 34° AND A VERTICAL (90°) SOLAR CHIMNEY ($T_{G, AVE}$), $D=0.25$ M AND $L_{ABS}=L_G=2$ M IN INDIA.	69
FIGURE 4.8: AVERAGE MONTHLY WALL TEMPERATURE ABSORBER $T_{W, AVE}$ FOR TILT-IN SOLAR CHIMNEY 34° TILT ANGLE & VERTICAL SOLAR CHIMNEY WITH $D=0.25$ M AND $L_{ABS}=L_G=2$ M IN INDIA.	70
FIGURE 4.9: INCLINATION ANGLE EFFECT ON AVERAGE MONTHLY ACH IN WINTER & SUMMER FOR INCLINED & VERTICAL SOLAR CHIMNEY WITH $D=0.25$ M AND $L_{ABS}=L_G=2$ M IN INDIA.	71

FIGURE 4.10: AIR GAP EFFECT ON AVERAGE MONTHLY HOURLY ACH FOR ROOF MOUNTED SOLAR CHIMNEY THROUGH INCLINED ANGLE OF 34° THROUGH $L_{ABS}=L_G=2$ M IN INDIA.	73
FIGURE 4.11: AIR GAP EFFECT ON AVERAGE MONTHLY ACH FOR WALL MOUNTED SOLAR CHIMNEY THROUGH $L_{ABS}=L_G=2$ M IN INDIA.....	74
FIGURE 4.12: CHIMNEY HEIGHT EFFECT ON AVERAGE MONTHLY ACH FOR ROOF MOUNTED SOLAR CHIMNEY WITH INCLINED ANGLE OF 34° THROUGH $D=0.25$ M IN INDIA.	75
FIGURE 4.13: CHIMNEY HEIGHT EFFECT ON AVERAGE MONTHLY ACH FOR WALL MOUNTED SOLAR CHIMNEY THROUGH $D=0.25$ M IN INDIA.....	76
FIGURE 4.14: VIEW FACTOR EFFECT ON AVERAGE MONTHLY COEFFICIENT OF RADIATIVE HEAT TRANSFER FROM ABSORBER WALL TO THE GLASS COVER (H_{RWG}) FOR ROOF & WALL MOUNTED SOLAR CHIMNEY THROUGH $D=0.25$ M AND $L_{ABS}=L_G=2$ M IN INDIA.	77
FIGURE 4.15: VIEW FACTOR EFFECT ON AVERAGE MONTHLY ABSORBER WALL TEMPERATURE FOR ROOF AND WALL MOUNTED SOLAR CHIMNEY; WITH $D=0.25$ M AND $L_{ABS}=L_G=2$ M IN INDIA.	79
FIGURE 4.16: VIEW FACTOR EFFECT ON AVERAGE MONTHLY ACH FOR ROOF & WALL MOUNTED SOLAR CHIMNEY; THROUGH $D=0.25$ M AND $L_{ABS}=L_G=2$ M IN INDIA.	80
FIGURE 4.17: VIEW FACTOR (VF) EFFECT ON AVERAGE MONTHLY ACH FOR VARIABLE AIR GAPS FOR ROOF MOUNTED SOLAR CHIMNEY WITH INCLINED ANGLE OF 34° AND $L_{ABS}=L_G=2$ M IN INDIA.	81
FIGURE 4.18: VIEW FACTOR EFFECT ON AVERAGE MONTHLY ACH FOR VARIABLE AIR GAPS FOR WALL MOUNTED SOLAR CHIMNEY WITH $L_{ABS}=L_G=2$ M IN INDIA.....	82
FIGURE 4.19: VIEW FACTOR EFFECT ON AVERAGE MONTHLY ACH FOR VARIABLE HEIGHTS OF CHIMNEY FOR ROOF MOUNTED SOLAR CHIMNEY WITH INCLINE ANGLE OF 34° AND $D=0.25$ M IN INDIA.	83
FIGURE 4.20: VIEW FACTOR EFFECT ON AVERAGE MONTHLY ACH FOR VARIABLE HEIGHTS OF CHIMNEY FOR WALL MOUNTED SOLAR CHIMNEY THROUGH $D=0.25$ M IN INDIA.	84

CHAPTER 1

1. INTRODUCTION

1.1 Safety of Energy

Another driver of natural ventilation is building energy security. Energy security may be called uninterrupted, economical, energy resources energy security. The Master Energy Security Plan of India ensures that energy security is at the disposal of the Indian economy for economic growth and poverty alleviation by providing various energy resources at sustainable quantities and affordable prices, into account environmental requirements and interaction between economies.

India faces an energy security crisis and electricity emergencies were declared in as well as in early 2020". "As fossil fuels are endless (non-renewable) energy sources, they will not always be available, so investment in alternative power sources is essential if energy security is to be ensured. Furthermore, the Indian economy is affected by this energy crisis as well".

1.2 Ventilation

To control the air chemical levels of humidity or temperature in this area, value is defined as the supply and air removal from every space. During the process of ventilation, air may or may not be affected. Ventilation is a dynamic part of the health, comfort, and productivity of its occupiers in many countries around the world. Ventilation standards have been established. The minimum volume of fresh air is estimated to be about 1.2 liters per second per individual, but for comfort level, the supplies must go outside to meet this minimum amount of oxygen requirement of the occupants, for odor dilution, carbon dioxide dilution levels, and, if applicable, minimize the increase in air temperature.

A ventilation building system is a key scheme criterion since it improves indoor thermal comfort and air quality. These factors depend upon this:

- Climate parameters and humidity, temperature, air velocity and air pollution levels.
- Occupant parameters like humidity, odors, carbon dioxide and tobacco smoke.

- Building parameters and outdoor bases, such as formaldehydes, organic volatiles, airborne substances, radon, and biological.

Ventilation can occur naturally in buildings. The wind or thermic buoyancy depends upon natural ventilation in order to move the air by external supply of energy.

1.2.1 Natural ventilation

To define as air movement due to properties of wind and thermal is called Natural ventilation as diffusion that may occur in a building via any intended openings. Difference of the temperature between inside & outside air increase to different air densities, resulting in pressure changes across the building's casing. Due to these pressure gradients, air movement is induced. Some openings for natural ventilation include doors, windows and fans or vertical streams in buildings. There are two main forms of ventilation available: stack and wind powered ventilation.

According to concept of wind effects, this type of ventilation operates. When a wind blows over a structure, it creates a 14-negative pressure upon that windward side as well as a positive pressure on the left side. Next, a pressure differential develops, which, in turn, influences the building's airflow. Wind-conducted ventilation depends on the mean driving pressure at opening & opening side to 3 fluctuating pressures [7].

A temperature difference between the inside and outside of a building causes stack-based ventilation. In buildings with higher interior temperatures, more air is drawn in and pushed out of the building, while the outside air stays colder.

1.2.2 The need for natural ventilation

Require power supplied largely from fossil fuels across the world through mechanical ventilation systems. Combustion of greenhouse gases with the fossil fuels produced by electricity. Greenhouse gas emissions grow leading to climate change Therefore, it is vital to minimize the consumption of fossil fuels in order to maintain the ecosystem. Natural ventilation encourages the long-term usage of energy since it is driven by renewable energy. Its main focus is solar chemistry, which is used in various applications throughout the world.

1.2.3 Drivers of Natural Ventilation in Buildings

Using natural ventilation in mostly building is considered as a more energy-efficient alternative to mechanical ventilation systems. To compare with conventional mechanical ventilation systems, natural ventilation in buildings offers various advantages [8].

1.3 Climate change

As a result of climate change, natural ventilation is also on the rise in the United States. Changes to climatic conditions "may be evidenced by fluctuations in mean or variability of its characteristics & may continue for a long period (typically decades) due to human activities or natural causes" are discussed in the second category [9]. Ocean heating in recent decades as a result of greenhouse gas increases has contributed to sea level rise. "Climate change is directly connected to rising greenhouse gas concentration in the atmosphere. Over the years 1993-2011, the global average level of water increased by 3.2 ± 0.4 mm per year, while since 1971, the mean global surface temperature is increased by 0.14 to 0.17°C per decade.

As the earth's temperature rises, the glaciers melt. Additionally, due to the excess heat storage & the loss of glacier mass caused by melting, an important contribution to marine growth comes from the ocean's thermal expansion. The level of sea level rise in the twentieth century was faster than the nineteenth century, and the rate of rise in the twenty-first century is expected to be much faster. Inundated coastal and lowland lands are degraded by rising sea levels.

Many types of studies conducted on the possible to climate change impact in the country with regard to India. Basing on long-term adaptation scenarios, the LTAs reveal that grassland biomes are most at-risk for major structural change owing to the invasion by woody plants as a result of rising temperatures & CO₂. Weather change has also been identified as a significant threat to the Nama Karoo habitat, the Indian Ocean shoreline, the Fynbos ecosystem, and the Forest biome.

1.4 Solar Chimney

As its name suggests, a solar chimney requires a fundamental function of the solar radiation. As a passive ventilation make cold system, a solar chimney is recognized as such. This consists typically of a glass wall, commonly called a glass cover, and an absorber wall parallel to each other, also known as a collector. The solar radiation can be passed through and absorbed in the collector through the glass cover. It also decreases the heat loss to convective air from the absorber wall. In contrast, the main purpose of an absorbent wall is to absorb the maximum amount of solar energy, to redesign the surface and to efficiently transfer heat to the domestic water. The working medium of solar chimney is air between glass cover and absorber wall of chimney.

Solar roofs & furnaces wall are the two forms of solar chimneys. As its names suggest, solar shakes on the roof of buildings and on the walls of buildings are mounted.

1.4.1 Wall-mounted solar chimney

A wall mounted solar chimney is like wall of Trombe. The latter absorbs solar energy and recycles hot air to ensure that buildings can be heated passively. However, in comparison with a solar chimney, the wall of Trombe has a massive thermal wall. Assumptions in the case of solar chimneys, it's a good thing undesirable heat stored behind the wall of absorber, as natural ventilation must be provided. Moreover, hot air is not recirculated in a solar chimney because hot air is excluded from the chimney. The solar-chimney installed in the walls of a building is given following fig. 1.1.

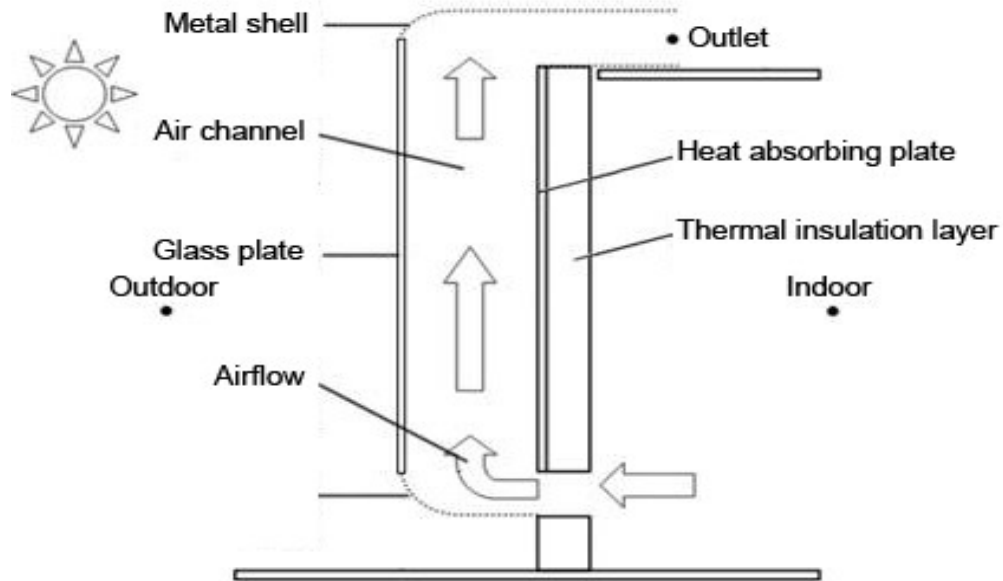


Figure 1.1 Wall Solar chimney diagram

1.4.2 Roof Solar Chimneys

Solar roof chimney can be fitted with gable roofs to ensure thermal comfort in the summer. Moreover, the using a solar collector effect on a roof under warm weather conditions on Europe styles in houses. The studies show that the sun's flow of energy is amount absorb by the house has decreased & the solar chimney provides natural ventilation that improves the thermal comfort of the home. The sunshade mounted on a building's roof is below given in Fig. 1.2.

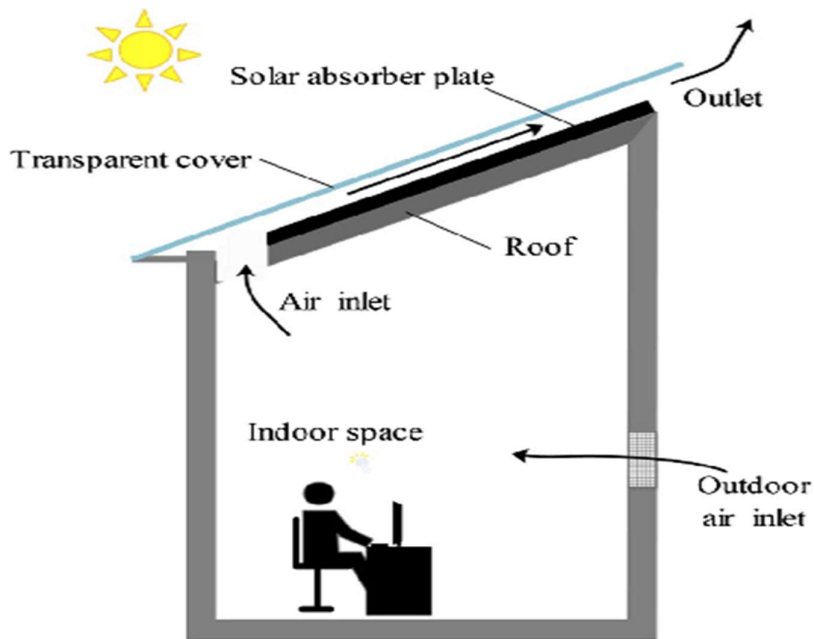


Figure 1.2 A Rooftop Solar Chimney Diagram

Through the absorbed in Solar Chimney, the sun gains thermal energy, which causes a substantial difference between inside & outside. The surface of glass is affected by the sun's rays, which are then absorbed by the walls of the absorber. The chimney generates a temperature differential between the air within the chimney and the air outside it by boosting flow of air thru the absorber wall.

In turn, this results to a pressure differential between the channel and the entry in the solar chimney, so that the hot air is evacuated from this chimney and the cooler air is pulled from the nearby area. The chimney has a large temperature differential. As outcome of the solar chimney, natural ventilation occurs in the room.

1.4.3 Parameters affecting the performance of solar chimneys

In order to study elements that impact solar chimney performance, several readings were taken from the solar chimney. Experimentally, practically & mathematically, some of those factors have been examined consist of solar radiation, Space between absorber wall & glass cover; height of solar chimney; degree of inclination; and glazing type are all factors to consider.

1.4.3.1 *Solar Radiation Intensity*

The solar radiation intensity is engine for design of solar chimney, which makes solar thermal the most important factor. With increasing solar radiation, solar energy temperature rises and the tower pressure rises.

The influence of sun radiation on ventilation rate was investigated. Using an iterative method, a numerical study revealed that ventilation rate rises with an increase in sun radiation. In experimental examined the heat flux effect on ventilation rate and compared experimental findings on heat-balance analysis with modeling of solar chimneys predicted outcomes. The heat flow ranges from 200 to 600 W/m² & increase in the heat flow, the rise in airflow rate. However, air flow quantities were less than indicated during the numerical simulation; nonetheless, the same pattern was seen numerical analyses indicated that ventilation rate improved as solar intensity improved.

Analysis of sun radiation's impact on ventilation rates. As a consequence of his research, He utilized a mathematical model to show that air mass flow rate increases with solar radiation. [10] A solar chimney numerical study using CFD computer software which showed that rate of venting rises with solar radiation intensity. Using the programming software from CFD carried out numerical tests on solar chimney performance. Increasing intensity of solar radiation raises the rate of ventilation. Solar chimney performance examined through CFD Programmed. The results of their numerical research reveal that when the intense solar radiation heights, maximum ventilation rate occurs.

CFD technology was studied for its influence on sun radiation levels. They have discovered that the mass of air flow rate increases as with increases of solar radiation. In both studies, an increase in intensity of solar radiation has been found to increase ventilation rate. The same trend was used the CFD to study solar chimneys.

1.4.3.2 *The air gap between glass cover & absorber wall*

According to CFD-technical numerical research, When the air gap was extended from 0.10 to 0.20 meter, the air flow rate went up from 0.1 to 0.2 meters. For small air gaps upstream from the solar chimney the air flow was seen but for significant air gap 0.5 m, due to abundance effects, the air flow was only upward by the heated absorber wall and

downstream along the solar chimney in the center. It's because in air areas that are greater than the two margins: the absorber wall and glass covering the inverse flow occurs.

The influence of ventilation rate of air gap both experimentally & numerically. They observed that increasing air gap with increases ventilation rate. Difference between the experimental findings and the simulated outcomes was around 10%.

It also numerically and experimentally studied ventilation rate is affected by air gap size [11]. The air gap varies between 0.1 and 0.6 m, and the solar radiation level is 400 W/m². Air flow rate is increased by an increased air gap but the experimental study could not establish an optimal air gap. Furthermore, a 0.3 m air gap was found in the reverse flow at the chimney's outflow. Reverse flow further below the solar chimney was seen when air separation rose from 0.3 m to 0.6 m. The increase in reverse flow unfortunately did not lead to a reduction of airflow, since the inlet of the chimney increased simultaneously and hence the pressure reduction at the inlet was reduced. Nonetheless an optimum air gap might be observed when inlet size for chimney remained constant as air gap was increased. The numerical study has also shown that air gap increases constantly, & no ideal air gap is seen. The numerical study has also shown that air gap increases constantly, and no ideal air gap is seen.

“[12] Air flow rises as the air gap widens, according to a numerical analysis. For simulation of solar chimneys CFD Programme was used. The air gap ranged from 0.1 to 0.3 m for solar radiation intensities of 300, 500, and 700 W/m². An increase in air gap resulted in higher in air flow rate for each and every amount of solar radiation. This is because an extensive air gap reduces the percentage of flow restricted by the limited layer, causing the air velocity to increase. The ventilation rate increases as the air gap increases. Their results were compared with approaches used for the review of numerical literature. Its experimental and computational findings have shown that the air gap rises and the heating rate keep going up. However, the numeration process actually predicts ventilation, especially for solar chimney with significant air vacuums.

1.4.3.3 *Chimney Height*

On a metallic solar wall, based on experimental and numerical analysis (identical to the solar chimney) “The impact of chimney height on ventilation rate was investigated

by researchers [13]. They discovered that when height of metal solar wall rises, rate of ventilation rises with it. “In an experimental and numerical research, [14] found that increasing chimney height resulted in enhanced ventilation”. The chimney was between 0.5 and 3 meters high. According to numerical analysis of solar chimney's performance & findings, Air flow rate increases as the height of the chimney grows. Performance of solar chimneys is influenced by height of chimney. They argued that venting rate increases with height of the stove because a longer path is taken between the absorber and the air stream for convective heat transfer. “As absorber wall surface rises with an increase in height of chimney, it has also been observed in research [15] that increase in height of chimney produces an increase in ventilation rate.” They utilized a mathematical model to solve problem. The impacts of chimney on solar chimney mounted on a roof were examined. The rate of ventilation rises with the height of chimney, according to their results.

1.4.3.4 *Inclination Angle*

The effect of inclination angle on solar chimney performance was investigated experimentally and statistically [16]. Their findings showed a maximum solar chimney flow rate of 1.5 m with a pitch of 0.2 m due to the incline angle of 45°. “Using CFD modelling tools, [17] studied the influence of a tipping angle on a flow rate of 52° for Edinburgh, Scotland”. The results revealed that maximum air flow rate could be achieved with a 67.5° inclination angle and a horizontal position. “Moreover, the influence of the inclination angle on ventilation rate is highly dependent on-site latitude [8]”. In Jodhpur, India, researchers investigated the effectiveness of solar chimneys and discovered that 45° inclination angle offered best air circulation, while inclination values of 30° and 60° generated equal results. Table 1.1 shows optimum solar chimney inclination angle at various latitudes.

Table 1.1: The optimal inclination angle varies with latitude [18].

Latitude (°)	Solar Chimney optimal inclination (°)
0	54
5	50
10	50
15	50
20	44
25	44
30	44
35	50
40	50
45	54
50	54
55	60
60	60
65	60

In addition, “[19] have been investigating inclination angle's impact on the solar chimneys' performance (2015) under Iraq's climate (33.3° latitude)”. The experiments and the numerical model for a solar chimney were proposed. From their numerical model, it was discovered that a 60° inclination angle provided best ventilation rate. Furthermore, “a number of studies by [20] found that the ideal angle of inclination for maximum ventilation rate is 45 degrees, with 32 degrees of latitude” [20]. They performed a numerical simulation in CFD to estimate the solar chimney performance.

1.4.3.5 *Type of glazing*

“Influence of glazing on performance of a solar chimney was quantitatively studied by [21] using CFD modelling techniques”. The advantages of double-glazing in greater ventilation rates, their results have shown. “The study also showed that the effects of glazing were significantly greater for low solar radiation intensities than for high solar radiation intensities. Indeed, the ventilation rates dropped by 11% and 35% respectively for solar radiations of 167 W/m² & 124 W/m², when double velocity is replaced by simple velocity. Furthermore, [22] used CFD modelling techniques to evaluate influence of glass on solar chimney performance”. The results show double vitrification provides a slightly

improved output than single vitrification. Nevertheless, since the progress was not significant enough, the use of double glazing was not cost-effective.

1.5 Solar Energy's Applications

Solar is a very heated gas sphere with diameters of 1.39×10^9 meters, around 1.5×10^{11} m from the Earth. In fact, the sun may be seen as an internal fusion reactor with component gases as a container held by gravitational forces during continuous operation. The Sun has around 73.88% hydrogen and 25% helium, while the rest are heavy elements which are neglected. Furthermore, it is calculated at around 5800 K for Sun surface temperature. A reaction in which four hydrogen atoms are combined to produce a helium atom is the main mechanism that sun provides for energy. The atomic mass of the helium is smaller than the total number of 4 hydrogen atoms. This corresponds with the mass-energy equivalence of Einstein, in which energy equals mass and square of the speed of light. For usage in the solar environment, ultraviolet, visible or infrasound regions with a visible radiation wavelength of 0.3 to 0.7 micrometers is very important for radiation released by the Sun.

Solar radiation may be transformed directly into energy or heat absorption for thermal solar usage via the photoelectric effect. There are many ways for collecting solar energy, including flat plates, evacuated tubes, concentrators and solar panels, to produce energy or heating.

1.6 Absorption of solar radiation as heat

To absorb solar heat as solar radiation, and transferring it into the system's working fluid (water or air). This is beneficial for producing hot water, such as solar water heating or natural ventilation through effect of building mounting. In solar thermal applications, a solar chimney is used.

The solar chimney uses in ventilation buildings allows for the employment of a passive cooling method. It employs sun rays to exchange heat through the movement of natural air. Thermal fluid is the airflow principle of device. Solar chimney air expansion raises temperature increases in solar chimney. This increase in air reduces air density, such that heated air gets hot and the chimney does seem to top.

Solar chimney is separated into two sections, vertical or inclined wall mounted Solar chimney & roof mounted solar chimney. A wall absorber, an air gap, and a glass wall are all common solar chimney components. It allows enough solar radiation to heat the natural upward flow of air, which is known as the chimney effect. Figure 1.3 depicts the layout of a solar chimney.

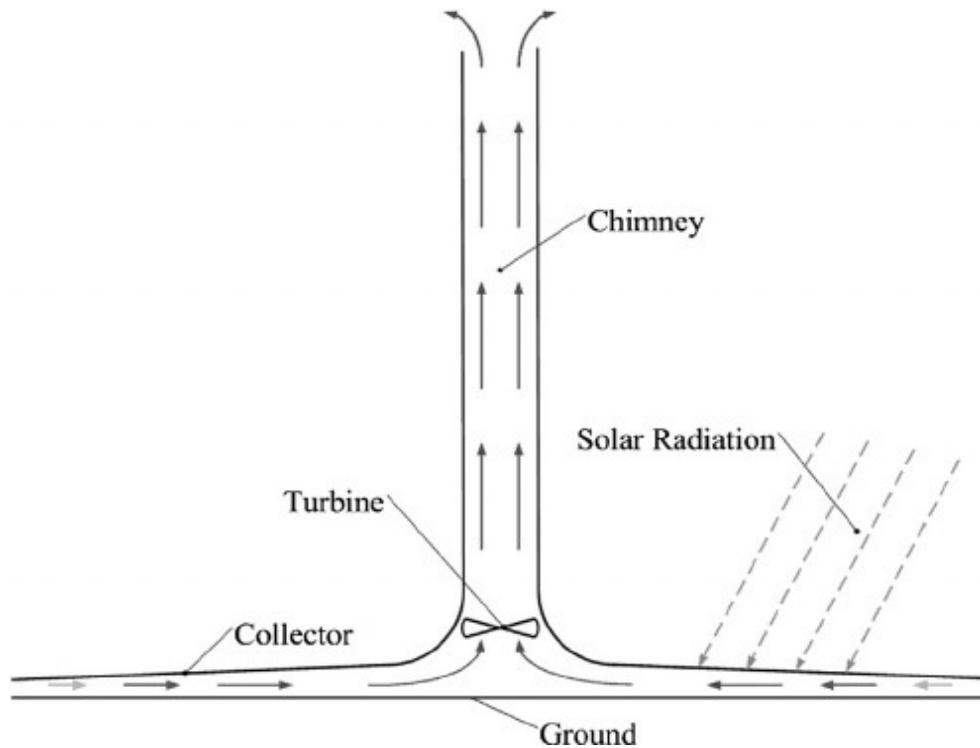


Figure 1.3 A solar chimney diagram

Figure 1.3 shows an example of this absorber wall & glass wall constitute main components. The solar chimney is where the collector absorbs sun radiation, heating the air. As air is heated, it raises & denser. The solar chimney draws air from the chamber by bringing warm air up to chimney top. This causes natural air flow from side to side the room through the solar chimney.

1.7 Thesis organization

There are 5 chapters in this thesis-

In Chapter 1 Some previous studies and research of natural ventilation are discussed.

Chapter 2 is a literature review on physics of solar chimneys and solar radiation. The review looks at heat transfer mechanisms and describes the Solar Chimneys in a comprehensive manner. There are also the problem statement, goals, and targets of this thesis.

Chapter 3 discusses the technique is chosen and the formula for the solar chimney mathematical model and simulation in CFD.

Chapter 4 gives the findings of the CFD simulation discussion and finds the outcomes.

In Chapter 5 provides conclusions & recommendation that on the basis of results & discussion. Follow in the context the references used in this study are listed, followed.

CHAPTER 2

2. LITERATURE REVIEW

In this Chapter, we define two principles of ventilation systems. The first is natural and the second is mechanical ventilation in buildings. Natural ventilation needs to focus on solar energy and some other solar energy applications are also discussed in this chapter. This chapter ends with a problem-defined statement. Defining goals and defining aims are also outlined. Finally, a thesis organization is included.

In this chapter, natural ventilation is introduced, the physics of solar radiation and solar chimney are investigated as well as geographic and astronomical concepts linked to solar radiation utilized in this study. In addition, modelling of solar radiation on tilted surfaces was discussed. There will also be a solar chimney detailed description. Discussion is also made of performance variables based on numerical studies of the solar chimney.

2.1 Some Previous Study

Most data used in the study have been obtained from the solar chimney is an interesting concept. Some prior research has been found on the usage of solar chimney in improving ventilation, with various designs. Some investigators wanted to analyze the vertical chimney, while others investigated the one-sided solar chimney.

This different set-up configuration was used according to the purpose of the study of solar chimneys. Solar chimneys were studied using a mathematical model. The numerical solution of the proposed model revealed an induced air flow range from 50 to 165 m³/s per square meter of collecting area for solar radiation values of 100–1000 W/m² on horizontal surface. This airflow is dependent on several factors including the collector geometry & cross-sectional area as well as performance characteristics such as top & bottom loss coefficients, absorptance and transmittance of collector plate glazing [1].

This is a research project that includes both theoretical and practical components. This evaluation of the utilization of sun or solar radiation in hot regions to induce room ventilation. The theoretical and experimental results of the created model were found to be

in good agreement. The airflow increases as the solar radiation or air gap between the absorber and the glass cover rises [2].

Offered an accurate way to improving inactive ventilation night in the collective casing through the application of the view of solar chimney. They have active and accessible, in-building construction high-thermal mass rather than fan-forced ventilation to capture solar power in their concrete walls during the evening (50°C). There was a separate chimney on top of each apartment with a swinging flap and the flap was closed during the energy gathering. At the night when the environmental temperatures dropped 20° about, the coverings on the top were opening to produce drainage via flats, cooling down thermal masses of roof [2].

Proposes to analyze a 0.24m concrete wall & at 2 m high solar chimney such as thermal storage energy. The original circumstances for the model were real Mediterranean climate data. After 2 hours than the ambient temperature, the concrete wall attained its higher temperature. In addition, following the start of the dark and inductive ventilation of night to maintain the temperature. The students proposed additional study on solar chimney thermal inactivity [3].

An experimental investigation was done on a test cell matching a real room size. They examined the influence of solar chimneys & water sprayed over a roof on natural ventilation. There was an average drop of around 3.5 degrees Celsius in temperature for individual chimneys, and an average of about 6 degrees Celsius for the combined impact of spraying with the sun's energy as well as with water spraying. On a related note, they observed that during periods of high solar radiation and ambient temperature, temperature differential between the entrance of the solar chimney and the exit tends to diminish. Alternatively, water spraying raises temperature differential & as a result, airflow rate via chimney. Further research should be conducted [4].

The solar chimney used to effect to improve the ventilation of natural was explored. They observed there was a connection between the inclination of the chimney height & absorber. Experiments values show that, depending on the place's latitude, the ideal absorber tilt angle varies from 40° to 60°. The trial or experimental data was related to recommended mathematical model & they discovered a virtuous concern.

To accompanied experimental research the influence of studying it that intensity of the solar varied like an electric heater, between 100 to 200 W/m² & mass flow rates across the passage was achieved by the conduit depth. There were recordings of temperatures and speeds and a correlation between mass flow rate and input as and channel depth was made to $m \propto S^{0.712}$ [5].

Different kinds of solar chimneys were compared in terms of performance. Evaluation of performance is the first step when a cylindrical fireplace is covered and uncovered. For the covered, mass flow rates improved. An angle of 45° was shown to be the optimal angle for a solar chimney compared to a vertical chimney [6].

As well as flow patterns in space, the previous study available do not show detailed data on the airspeed supply when flows of air through the chimney. Furthermore, the advanced rate of flow correlations with depth & intensity of chimney has not been validated. The focus of this thesis is therefore on studying effect on flow pattern of air velocities down chimney from the ground of room, the air gap between the absorber & glass. It also seeks to show airflow patterns under various operational circumstances.

2.2 Problem Statement

Building accounts for 32% of global final power consumption by (IEA 2020). More than a third, it appears the total amount of energy consumed and the resulting greenhouse gas emissions in countries also come from buildings. The heater, cooling and ventilation is primarily used for this energy.

The building sector significantly contributes to greenhouse gas emissions resulting from combustion of electricity generated by fossil fuels. Climate change is also the consequence of greenhouse gases, which has undesirable environmental effects. Furthermore, waste wastes such as coal fly ash, which is produced during the burning of fossil fuels, are a significant environmental concern. Moreover, the finite sources of energy are fossil fuel, to investigate ways of minimizing energy consumption in constructions. One such strategy is the installation of solar chimney on building roofs or wall. “Natural ventilation is one of the most important design criteria for buildings, since it offers unique

advantages over mechanical ventilation systems in terms of energy consumption and environmental effect [23].” Solar chimney is furthermore said to receive universal responsiveness because of its potential to reduce heat recovery and induce ventilation without harming the environment. Solar chimneys have been the subject of several numerical and experimental research to determine their performance in various temperatures and design factors. Prior research into solar chimneys, Alternatively, the view factor is one of the most frequently ignored variables. A prior study has never addressed the effect of the view factor on performance of solar chimney. As a consequence, it's essential to look at the thermal efficiency of walls and roof-mounted solar panels in terms of which buildings would be more effective, as well as the impact of the view, which has been overlooked in earlier research.

2.3 Literature Review of Mathematical modelling

The most numerous permanent sources of energy have been established. Solar power. As the Solar Chimney idea is based on solar radiation and thereby reduces the emissions of GHG, it receives a lot of global importance. Numerical studies have been performed to map solar chimneys on walls and towers, as well as numerical experiments.

“In 1993, [24] created a mathematically stable model to numerically evaluate the effects of ambient temperature & solar radiation on solar chimney mass flow rate.” An iterative procedure used to resolve the mathematical model. A numerical studies of solar chimney performance based on CFD techniques were carried. To validate their model, they used experimental data to compare results of their numerical simulation. “[25] presented a mathematical model to investigate performance of a metallic solar wall under Bangkok climates in Thailand.” The model was resolved using the Newton-Raphson technique, and tests with the metallic solar wall were carried out to compare numerical results with experimental results.

The theoretical investigation on a combined solar chimney wall roof was performed, to determine the ventilation speed and an optimum height of the solar chimney wall. A thermal model that combines Equations for heat transfer and natural ventilation flow for solar chimney simulation have been designed. In order to solve their mathematical model, they used a finite different method. In the area of Porto, Portugal they also

conducted experiments with solar chimneys to compare their model results with experimentally obtained results.

A mathematical solar chimney-based model based on the continuous transmission of heat. In terms of avoiding efficacy of a solar chimney, the equations created by their model were solved using the reverse-matrix technique. To research air gap effect & the intensity of solar radiation on solar chimney efficiency. They also performed experiments to establish a mathematical model of a solar chimney with a height of two meters as well as a width of 0.45 meters.

“On basis of 1-D, consistent heat transfer,[24] developed a mathematical model for determining airflow speed in solar chimney.” In order to solve their model equations, they employed CFD software. They evaluated their model on a physical prototype of a solar chimney. “[26] also investigated effects of air gap & absorber wall height on ventilation rate using a model similar to [27].” They also conducted experiments on a solar chimney physical model and compared results of the experiments against the values derived from the mathematical model of steady state. To look into the functioning of solar chimneys from a variety of angles. To compare numerical and experimental results, they tested a physical model of a solar chimney.

“Solar chimney uses being researched to minimize thermal load in office buildings was carried out in Japan under Japanese climatic conditions [28]”. They calculated heating and cooling expenses using CFD modeling techniques. In addition, a physical model for solar chimney thermal performance under Mediterranean climate conditions was presented. This model was created using an unstable thermal transmission taking into account the solar chimney's thermal inertia. This model's set of equations have been solved by an iterative procedure who have used to Analyze inclination angle impacts mathematically & vitrification on ventilation rate.

A mathematical model based on the heat transfer processes that occur within solar chimney system. A mathematical approach for determining ideal tilt angle for maximum ventilation rate in a solar chimney. In their study, they used solar radiation data to solve equations from their mathematical model using the CFD software. To investigate the effects of chimney height, air gap, absorptive absorption of the wall, and transmission of

the glass coverings on solar chimneys under various climatic circumstances using numerical simulations.

A mathematical model of a Solar Chimney in steady-state was employed to solve mathematical model equation applied by CFD program software is the ability to numerically study the impacts of a wall height, breadth, intensity, air inlet speed, air inlet ratio and outlet area.

To enhance the design of a multistory solar chimney. They also used test data to the performance of solar chemists using CFD computer software was numerically investigated to the place chosen for her numerical study. The energy balance equations were used in model, the absorbers wall & air within the solar chimney channel and used a constant state mathematical model. To model heat dynamics on the roof of a solar chimney. A one-dimensional static distribution of heating across the system has been established for the solar panel's mathematical model. The influence on solar chimney performance in climatic conditions was quantitatively studied by the inclination angle & the relationship between the height & the air gap of absorber. They applied their mathematical model in the CFD software and experimented with to compare numerical data with actual data, a physical model of a solar chimney. Airflow mode related to natural convection in the solar chimney has been studied in a numerical simulation. The later was modelled as an excessively heated air flow on absorber wall & glass cover. The effect of chimney Hight & wall areas on performance of roofed solar chimney was also digitally investigated using CFD software. They devised a mathematical model for transmission of heat in a continuous manner.

“[29] statistically and experimentally studied the solar chimney performance in Iraqi climatic condition.” They created a CFD-solved two-dimensional mathematical standard model. To examine the solar chimney fluid's dynamic and thermal performance, a 3-D mathematical model was created. To solve their mathematical model, they use the CFD modelling techniques.

2.4 Scope of study

The solar chimney's thermal efficiency is examined on the roof and on the wall under the same environmental factors. Different factors were investigated to enhance the

thermal performance chimneys. Only theoretical study is confined to practical experiments not done. However, in order to establish mathematical model developed in this study, numerical data from this thesis was compared with experimental literature data. To simulate various CFD software system parameters.

2.5 Aim and Objectives

This study is to evaluate the thermal efficiency in terms of ventilation rate for solar roof and wall chimney.

The study's particular objective is to:

- Solar chimney designing on the roof and wall.
- The mathematical model for solar chimneys is to be developed and validated.
- Simulation of solar chimney thermal performance.
- Determine the solar chimney's most efficient structure.

CHAPTER 3

3. METHODOLOGY

Due to the popularity of solar chimneys as natural ventilation in buildings, several experimental and computational investigations have been undertaken. Chapter 2 discussed the introduction of solar chimneys. The thesis shows some different observations regarding the performance of solar chimneys. To have a better understanding of solar chimney performance, more study is required. The methodology and formula for this study are discussed in this chapter. A mathematical model for the solar chimney was built based on prior solar chimney research and the models generated. To address the problem, the system of mathematical model equations, a program was then written in CFD computer software, numerically examining the thermal performance of several solar chimney configurations.

3.1 The primary energy source for electricity generation

The major energy source for generating power is mostly fossil fuels. The global electricity generation per source is shown in Figure 3.1. (International Energy Agency [IEA], 2020). As Figure 3.1 shows, 61 percent of worldwide power generated by coal, oil and natural gas.

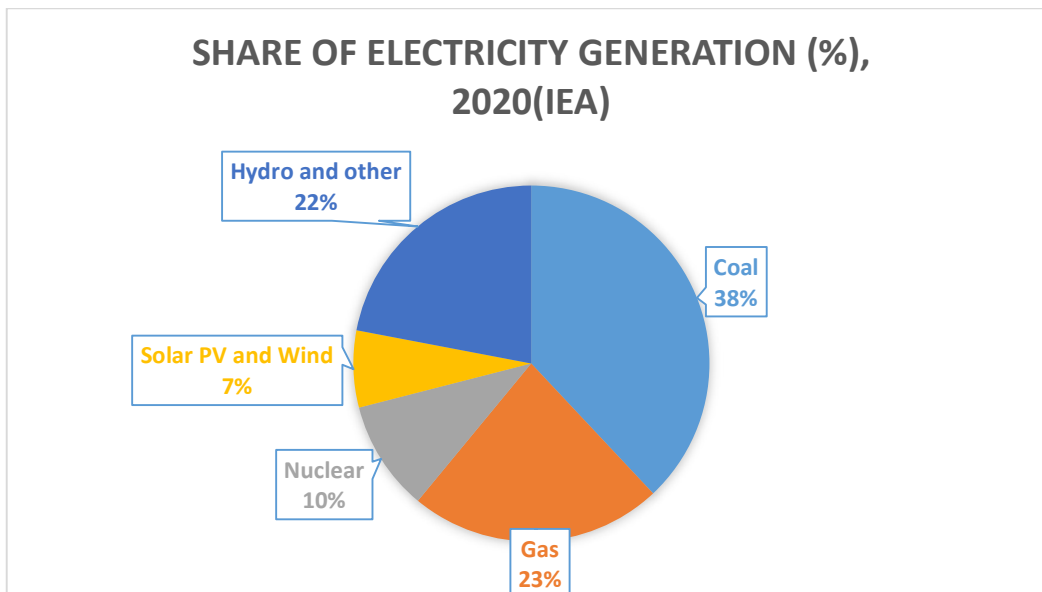


Figure 3.1: In 2020, the global power generated by each energy source will be calculated, IEA (International Energy Agency) (2020).

"The building industry has been one of the most resource sectors of the economy." Fig.3.2 illustrates how buildings and other industries will contribute to global final energy consumption by 2020. Construction made up 27% of the final energy intake by 2020 and, as indicated in figure 3.2, this is the greatest percentage of final energy in all sectors.

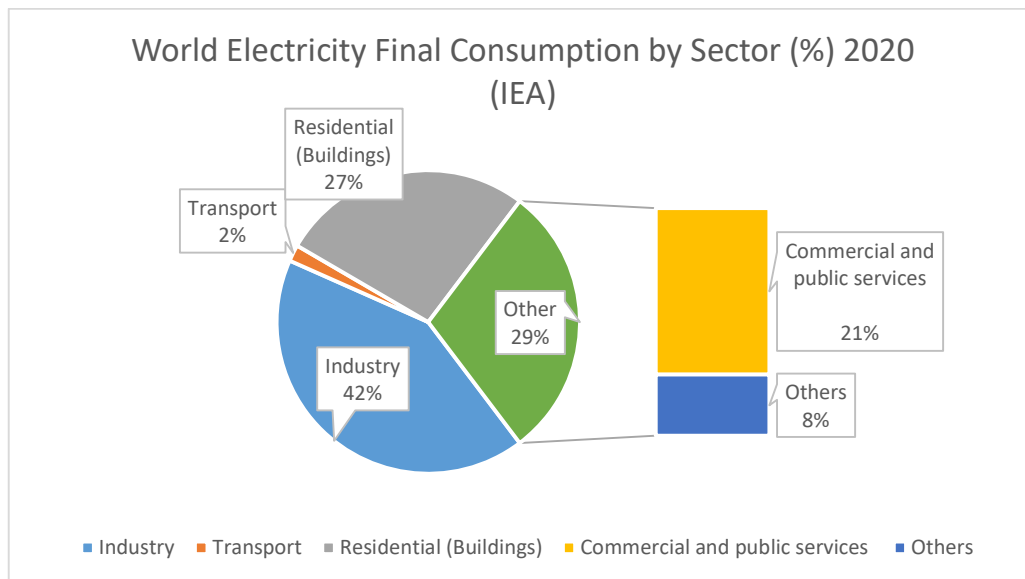


Figure 3.2: In 2020, residential (buildings) and other sectors will use a larger percentage of global final energy consumption. Agriculture and other unspecified sectors are among the others. Adapted from the International Energy Agency (2020)

The main focus is India, and so analysis of the energy sector in the country is essential. The percentage of power generated in India by energy source is depicted in Figure 3.3. The country relies heavily on coal to generate electricity 88.80 per cent of the total power generated in 2020 was actually derived from coal, as shown in Fig. 3.3 (IEA, 2020).

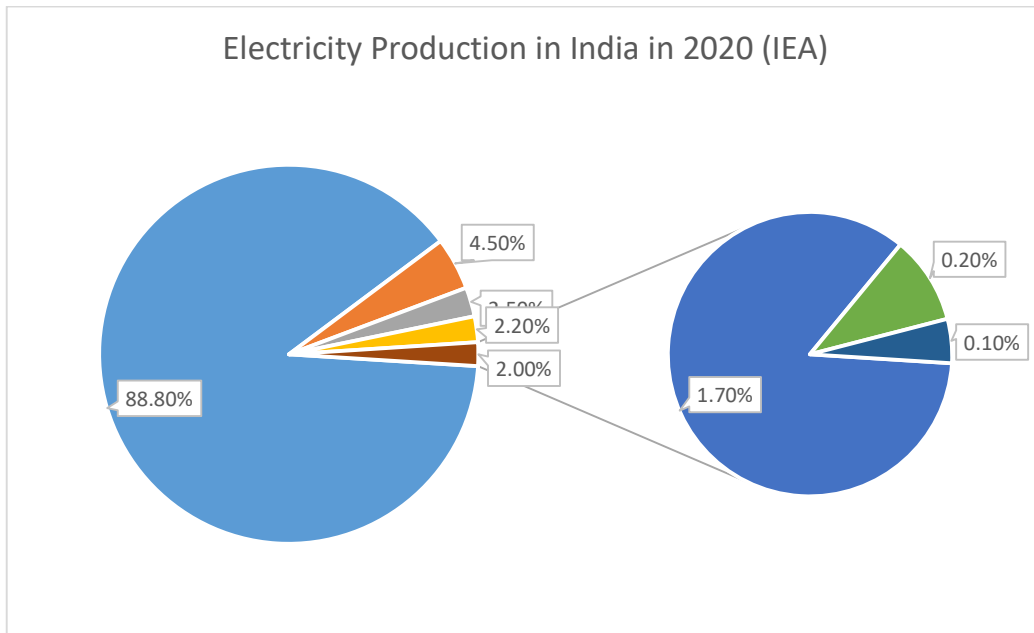


Figure 3.3: India's electricity generation by fuel type in 2020. Adapted from IEA (2020)

The final energy consumption of Indian buildings in the year 2020 is shown in Figure 3.4. Residential buildings were projected to consume about 3.4 Mtoe (20%) in 2020 while transport consumed about 0.3 Mtoe (2%) in 2020; thus in 2020 the building industry was consuming in India a productive use of (78%) 13.3 Mtoe of final power (IEA, 2020).

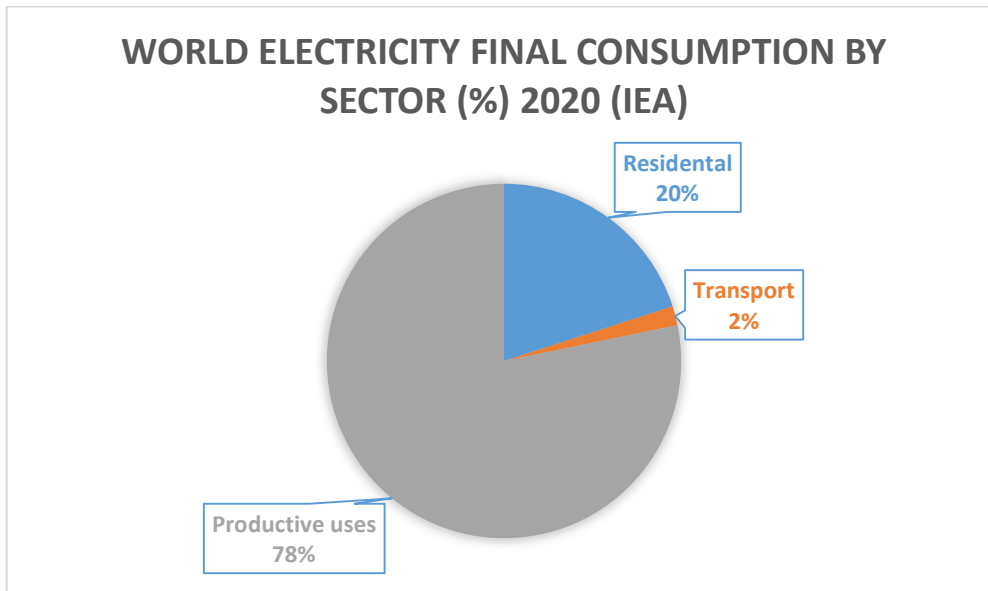


Figure 3.4: India's final energy usage in the building sector. Source: IEA (2020)

National and international level in general observation, the large quantities of energy consumed by the building sector. Fossil fuels are heavily used to generate electricity worldwide. The application of renewable energy in buildings is important. The only way to decrease the use of power by mechanical ventilation is to employ natural air ventilation in construction.

3.2 Solar radiation Physics

“Radiated solar chimney to Earth's surface with components mainly from the electromagnetic spectrum regions of the visible, infrared and ultraviolet regions”. The first is beam radiation, and the second is diffuse radiation, known as diffuse radiation. The term "global radiation" refers to all direct and diffuse radiation. A pyrhelimeter is often used to quantify normal radiation in the incidence beam, whereas a pyrometer is typically used to measure total radiation.

Using pyrhelimeter, global radiation measurements on the surface are made because of a hemispheric viewpoint of the environment, whereas a pyrhelimeter gives a concise review.

3.2.1 Direct radiation

The radiation that arrives without atmospheric dispersal from sun is defined by direct radiation or radiation via beam. On the surface of the Earth, it does not change direction. Figure 3.5 depicts solar radiation as direct radiation.

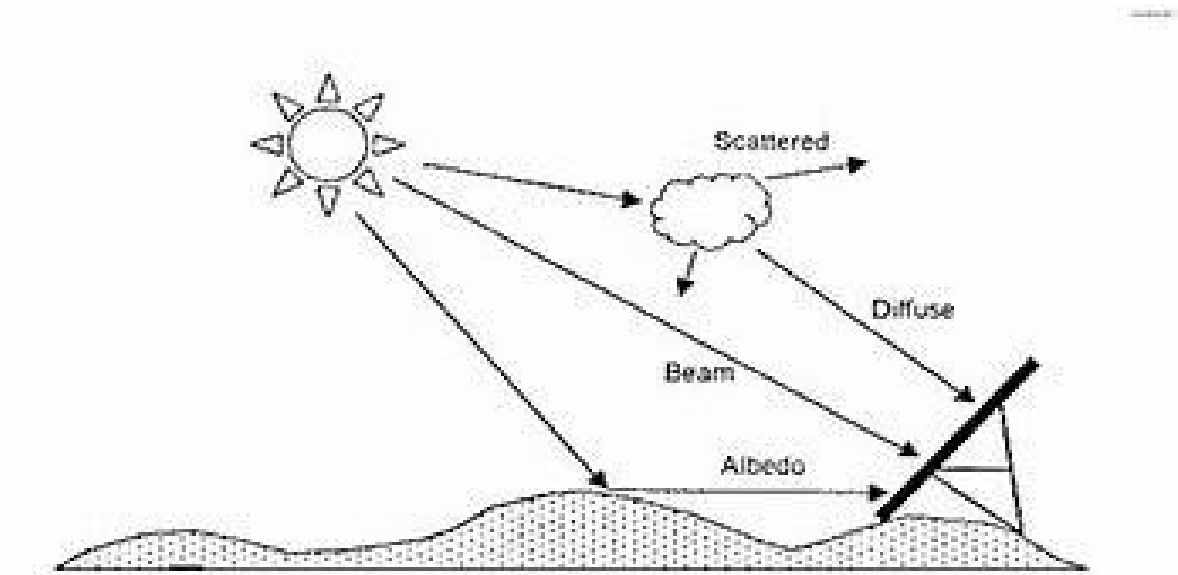


Figure 3.5: Beam radiation on a slanted surface.

3.2.2 Diffuse Radiation

Radiation that has been dispersed or diffused According to the definition, light is defined as solar radiation that reaches surface of earth after passing through atmosphere, and diffuse radiation is generated by four main phenomena.” When direct radiation meets oxygen and nitrogen molecules in atmosphere, the radiation is spread in all directions. In short wavelengths, this impact is more noticeable. Secondly the blue sky, water vapor molecules in the atmosphere disperse direct radiation. Thirdly, there is also selective absorption, which results in diffuse radiation, by ideal gases and water vapors. Fourthly, the dust particles into the atmosphere leads to diffuse radiation. The illustration of diffuse radiation is given in Fig.3.6.

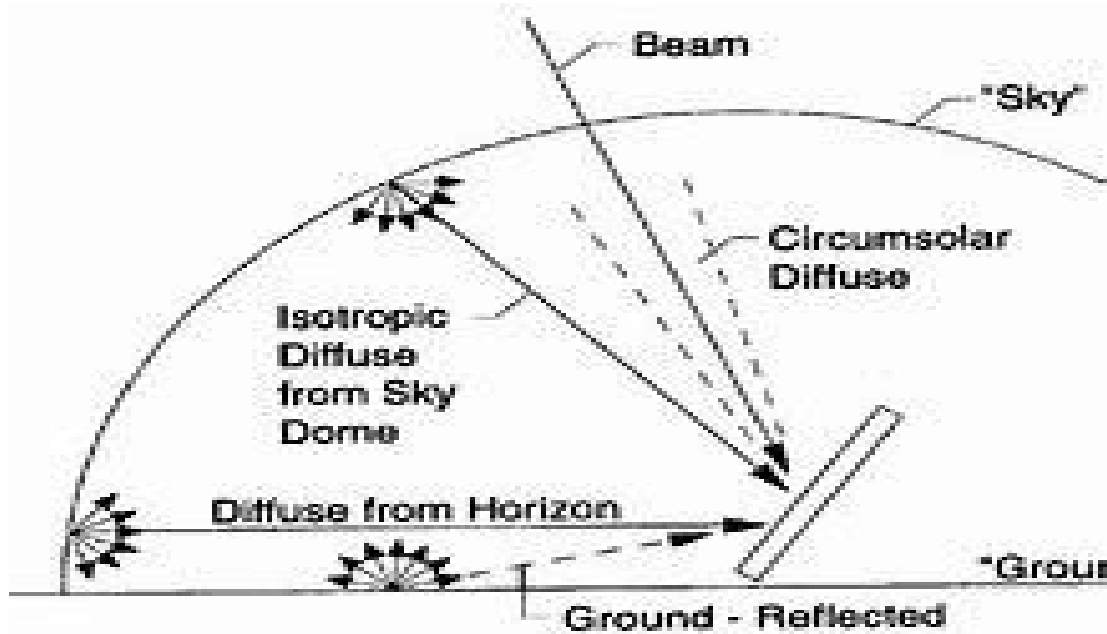


Figure 3.6: Diffuse Radiation on a tilt surface

3.2.3 Parameters of Geographical & Astronomical

The sun radiates an overall energy output of 3.8×10^{20} MW in all directions, although only a small portion of the surface of earth is impacted. The entire quantity of energy emitted by the sun that has reached the Earth's surface is about 5.46×10^{24} MW annually, according, but the total annual electricity required to meet the annual global energy requirement is just around 0.01 per cent. Despite this, the Earth's surface does not dependent heavily on amount of solar energy received as well as earths and its unique geometry. Many geographic and mathematical terminology linked to the relationships of the Earth sun are used in this research, detailed in the following sections.

3.2.4 Latitude and longitude

Determine any location on earth's surface by two coordinates latitude and longitude. The angular position of a location on surface of earth in relation to equatorial plane is referred to as the latitude of the site. A positive latitude value indicates that site is situated in South and positive value that the site is located in South. Conversely, in England Greenwich, the length of a place is always specified with reference to the nullification line.

The zero-longitude line is usually called the Greenwich Meridian, and the lengths are usually east or west of Greenwich Meridian. A positive longitude value implies that place is east of Greenwich meridian, and that the positive value is east of Greenwich meridian.

3.2.5 Declination Angles

The angle formed by the line between the sun and the earth's center with its projection on the equatorial plane. This is called declination angle and it is representing δ , it is due to the tilting of earth. In this thesis the convention is as follows: The South angle of the equator refers negatively and the north angle of equator refers positively and n is numbers of days. The angle of decline can be calculated in:

$$\delta = 23.45 \sin \left\{ 360 * \frac{(284+n)}{365} \right\} \quad (3.1)$$

Where n = day of the year; $1 \leq n \leq 365$.

However, equation (3.2) provides a more accurate equation for determining declination angle:

$$\delta = \frac{180}{\pi} (0.006918 - 0.399912 \cos B + 0.070257 - 0.006758 \cos 2B + 0.000907 \sin 2B - 0.002697 \cos 3B + 0.00148 \sin 3B) \quad (3.2)$$

$$B = (n - 1) \times \frac{360}{365} \quad (3.3)$$

3.2.6 Solar Time

The solar time is another important. At a given position, Solar Time is actual time according to the sun location is termed as solar time & watch time or standard time is defined that the time at standard longitude of country as per sun location. The solar time may be used as an equation (in minutes):

$$\text{Solar time} = \text{Standard time} + 4(L_{st} - L_{lo}) + E_{time} \quad (3.4)$$

Where L_{st} and L_{lo} refer to the standard meridian longitude and local longitude respective length. Standard time by increasing the time difference between the time of standard longitude and local longitude by 15 to add watch time. E_{time} stands for the time equation, which is written as follows:

$$E_{time} = 229.18 (0.0000075 + 0.001868 \cos B - 0.032077 \sin B - 0.014615 \cos 2B - 0.040849 \sin 2B) \quad (3.5)$$

3.2.7 Hour Angle & Sunset Hour Angle

The Hour angle, shown by ω average 15 degrees an hour is a shift from local longitudinal line by earth rotating on its own axis.

$$\omega = 15 \times (\text{solar time} - 12) \quad (3.6)$$

Another parameter used in this thesis is the sunset hour angle (as in the case of sunset hours). It depends on the location's latitude and the angle of decay. The angle of sunset time is as given.

$$\omega_{ss} = -\tan \phi \tan \delta \quad (3.7)$$

3.2.8 Solar Zenith Angle & Surface Azimuth Angle

The Solar Zenith Angle (θ_z), it is vertical angle between beam's rays' direction & line perpendicular horizontal plane direction of the Sun in the sky:

$$\cos \theta_z = \sin \phi \sin \delta + \cos \phi \cos \delta \cos \omega$$

Other the surface angle azimuth indicated by γ is called horizontal angle between the projections of normal vector from surface to the southern direction of the earth.

3.2.9 Incidence angle

The angle at which a beam of radiation strikes a surface, symbolized as θ_1 , defined that vertical angle between beam radiation direction & normal vector from inclined surface and is a function of declination angle (δ), latitude of location (ϕ), surface azimuth angle (γ), hour angle (ω) & slope or tilt angle (β). Cosine of incidence angle can be expressed following:

$$\begin{aligned} \cos \theta_1 = & \sin \delta \sin \phi \cos \beta - \sin \delta \cos \phi \sin \beta \cos \gamma + \\ & \cos \delta \cos \phi \cos \beta \cos \omega + \cos \delta \sin \phi \sin \beta \cos \gamma \\ & \cos \omega + \cos \delta \sin \beta \sin \gamma \sin \omega \end{aligned} \quad (3.8)$$

3.2.10 Albedo

The reflectivity of a solar radiation surface is specified as that of the surface albedo. This is ratio of solar radiation reflected to total surface radiation. This parameter, called ρ_g , is used to evaluate the radiation reflected by the earth that is used into calculate total solar radiation on a sloping plane.

3.3 Solar radiation modeling on inclined planes

To determine total solar radiation collected on the slope surface, a number of equations must be solved. In these equations, serval terms are used and discussed in the following points.

3.3.1 Solar constant

The solar constant, which is called GSC, is defined as the average sunlight collected at an average distance from Earth from Sun on a surface perpendicular to solar beams outside environment. The solar constant has value of $1366 \pm 3 \text{ W/m}^2$, but solar constant has value of 1367 W/m^2 at World Radiation Center. For all computations, this thesis thus utilized value of 1367 W/m^2 .

3.3.2 Extraterrestrial Solar Radiation

Extraterrestrial solar radiation I_o , is premise that solar energy emerges in a horizontal plane on Earth's surface without an atmosphere. In a horizontal extraterrestrial plane, the following may be determined at any moment throughout the day:

$$I_o = GSC * \left[\frac{1 + 0.033 * \cos \cos (360n)}{365} \right] * \cos \cos \theta_z \quad (3.9)$$

3.3.3 Solar radiation on a tilt surface: beam, diffuse & ground reflected

On a tilted surface, whole sun's radiation, namely beam ($I_{b,t}$), diffuse ($I_{d,t}$) and floor-reflected radiation, can be expressed as a sum of three components. The level of diffuse and global radiation on horizontal surfaces is generally measured, thus the solar radiation on an inclined surface comes from transforming the solar radiant into a sloping area.

Sun radiation may be represented as a total of three components on a slanted surface, i.e., Beams ($I_{b,t}$), diffuse ($I_{d,t}$) and floor reflected radiation. The solar radiance in a sloping surface is due to the solar radiant being converted into sloping area, while the amount of diffuse and global radiation is generally measured on the horizontal surfaces.

The geometric factor is an important parameter used in calculating sunlight in the inclined plane (R_b). Later, the ratio of radiation beam on an inclined plane to radiation beam on a horizontal plane (I_b) is defined at all time.

$$R_b = \frac{I_{b,t}}{I_b} = \frac{\cos\theta \cos\theta_z}{\cos\theta_z} \quad (3.12)$$

The intensity of the beam radiation on an inclining plane may be determined using the following equation by multiplication the beam radiation component by means of a horizontal surface with the geometrical factor:

$$I_{b,t} = I_b R_b \quad (3.11)$$

Different models were developed for estimating diffuse solar radiation on sloping surface. Some are isotropic and some are anisotropic in nature. Isotropic analysis is predicated on assumption that radiation intensity of the sky is diffuse and homogeneous. Anisotropic models, however, have in mind the non-uniformities of diffuse sky radiation close to sun surface & isotropic diffuse radiation from remainder of sky structure. Figure 3.7 depicts the components of solar radiation on a sloping surface.

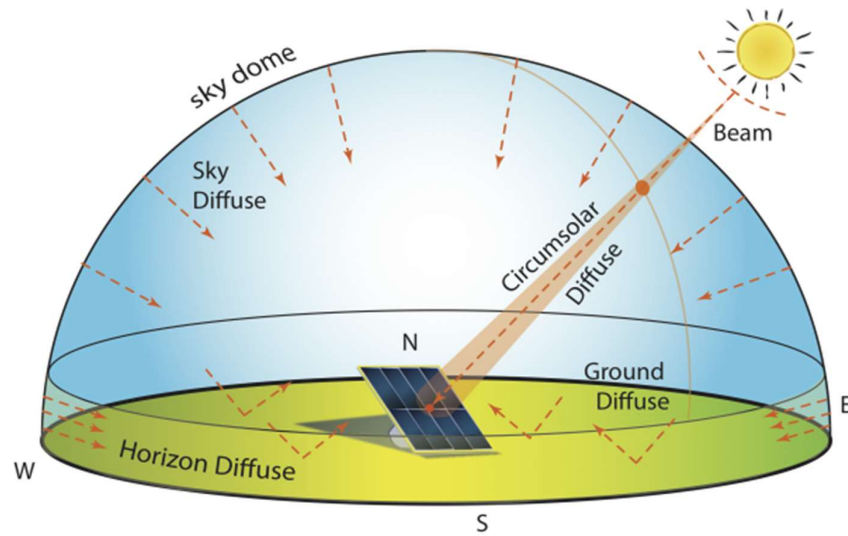


Figure 3.7: Components of Solar radiation on tilt surface

The diffuse Solar radiation on the sliding surface was observed to consist of three parts, i.e., a diffuse isotropic component derived evenly from a dome; the alignments, diffuse element obtained from the forward transformation of a light solar radiation; and the luminous, most apparent, horizontal component from clear sky and showing those diverse components. A brief overview of a few models of solar radiation is provided in Table 3.1.

Table 3.1: Models of Solar Radiation [18]

Models	Description & equation
Liu-Jordan (1961)	Assumes isotropic diffuse radiation: $\Psi = \cos^2 \left(\frac{\beta}{2} \right)$
Temps-Coulson (1977)	Assumes a clear sky: $\Psi = \cos^2 \left(\frac{\beta}{2} \right) \left[1 + \sin^3 \left(\frac{\beta}{2} \right) \right] \left[1 + \cos^2 \theta \sin^3 \theta z \right]$
Hay (1979)	The isotropic and circumsolar diffuse radiation components are assumed to be linear: $\Psi = A_i R_b + (1 - A_i) \cos^2 \left(\frac{\beta}{2} \right)$

At an earlier stage in this thesis, the various symbols used in Table 3.1 were defined and the new criteria are following:

Ψ the ratio of diffuse radiation to horizontal diffuse radiation on the tilted surface.

A_i is anisotropic index for transmission of the radiation beam atmosphere which can be expressed as follows:

$$A_i = \frac{I_b}{I_o} \quad (3.12)$$

The horizon lightening was taken into account including a $1 + \sin^3(\beta/2)$ correction factor. In order to account for cloudiness, revised this correction factor to incorporate a modulating factor, also added to the Hay model a similar term provide this modulation factor:

$$f = \sqrt{\left(\frac{I_b}{I_g}\right)} \quad (3.13)$$

Where, I_g = Global Solar Radiation on horizontal surface.

The following is a representation of equation:

$$I_{d,t} = I_d \left\{ (1 - A_i) \left(\frac{1 + \cos \cos \beta}{2} \right) \left[1 + f \sin^3 \left(\frac{\beta}{2} \right) \right] + A_i R_b \right\} \quad (3.14)$$

The above equation was used in this study to estimate diffuse solar radiation on a tilted surface because horizontal brightening and cloudiness are improved over the isotropic model. The equation for the third component of solar radiation on an inclined plane, soil reflection, is as follows:

$$I_{g,r} = \left(\frac{1}{2} \right) * \rho_g \times I_g \times (1 - \cos \cos \beta) \quad (3.15)$$

As a result, the total solar radiation on an inclined plane may be represented as:

$$I_t = I_{b,t} + I_{d,t} + I_{g,r} \quad (3.16)$$

The following equation can be used to express equation (3.20) explicitly:

$$I_t = (I_b + I_d A_i) R_b + I_d (1 - A_i) \left[\left(\frac{1 + \cos \cos \beta}{2} \right) \times \left[1 + f \sin^3 \left(\frac{\beta}{2} \right) \right] + \rho_g \times I_g \left(\frac{1 - \cos \cos \beta}{2} \right) \right] \quad (3.17)$$

Theoretical knowledge of thermodynamics and heat transport is also required to comprehend the idea of solar chimney operation.

3.4 Design of solar chimneys

Solar chimneys must be constructed to maximize solar energy absorption to maximize ventilation rate. Typically, the solar chimney consists of four walls, the two walls and the glass wall create a duct by means of which air is moved by natural convection and the wall is formed of glass (usually a glazed cover), a wall considered to be black (the wall of the absorber) and the two other walls. The air gap is defined as space between the levels of various geometric levels & the absorber wall is parallel to the glass cover.

A number of criteria are designed to take into account, including the chimney height, air vacuum, type of absorption device and the solar chimney's insulation, glazing & thermal size. A crucial design parameter is the difference in temperature between the intake & exit of solar chimney. The roof or wall can be equipped with solar chimneys. The model for this solar chimney installed on the wall of study is shown in Fig. 3.8. The temperature of different solar chimney components is also indicated in Figure 3.8.

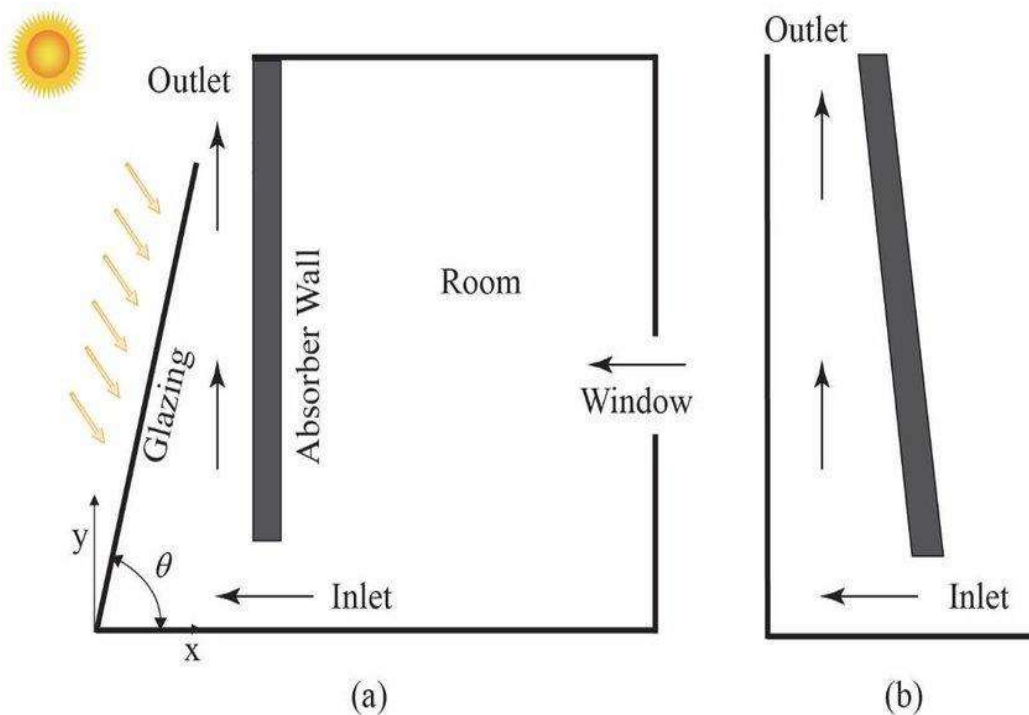


Figure 3.8 (a) & (b): Solar chimney mounted on a wall

As Figure 3.8 shows, the vertical wall-mounted solar chimney has a 90° inclination to a horizontal position. A horizontal structure equivalent to that of the absorber wall is connected to a glass cover. The length and width of the glass cover & absorber wall are 2m * 1 m. The insulation thickness is 0.1 m and the distance between the air & absorber wall is 0.25 m. Solar chimney entry is about 0.1 m in height and the airflow region is around 3 m * 3 m * 3 m.

The glass cover's surface is passed to the wall of absorber when sun radiation strikes it. The solar energy is subsequently collected and transformed into heat and transmitted Through convection to the solar chimney tube's air stream. When air is heated, the solar chimney's density is changing and the amount of air that is intake of solar chimney is changing. This density difference occurs in pressure differential, which removes hot air from solar chimney & low pressure.

The roof-solar chimney, and from the other hand, was inclined to a horizontal level at 34°, but the size of the vertical wall was the same. The solar chimney on the roof is on same basis principles as wall mounted solar chimney.

3.4.1 Design parameters of solar chimneys

3.4.1.1 *Location*

In India city in the Rajasthan in the Northern hemisphere, was considered in connection with this study. Jodhpur Rajasthan has a latitude and longitudinal of 26°16'6.28"N, 73°0'21.38"E. Figure 3.9 shows where in Jodhpur India.



Figure 3.9: Location of Jodhpur India

3.4.1.2 *Orientation of solar collectors*

The solar collector is directed at the equator in order to maximize solar radiation absorption that means that solar collectors should be facing south and solar collectors in the North, according to this study. This analysis consequently assumed that solar chimneys were faced south to take the most energy available during the day.

3.4.1.3 *Inclination angles*

The inclination angles for a roofed solar chimney were 30 degrees, 34 degrees, 45°, 60°, 75 degrees, and for a walled solar chimney 90 degrees were observed. The link between optimum inclination angle of the solar panel & location latitude (ϕ), as seen in Table 3.2 showed, has been identified in several research.

Table 3.2: Optimum tilt angle for Solar Collector [18]

Source	Optimum tilt angle of solar collector
Duffie & Beckman (2013)	$\phi \pm (10^\circ \text{ to } 15^\circ)$
Heywood (1971)	$\phi - 10^\circ$
Lunde (1980); Garg (1982)	$\phi \pm 15^\circ$
Chinnery (1971); Kern & Harris (1975)	$\phi + 10^\circ$

Löf and Tybout (1973)	$\phi + (10^\circ \text{ to } 30^\circ)$
Hottel (1954); Yellot (1973)	$\phi + 20^\circ$
Elminir et al. (2006)	$(\phi + 15^\circ) \pm 15^\circ$

Different correlations define that between the various sources and the optimal tilt angle for winter & summer seasons can be observed. A fixed tilt angle of solar chimney overall year-round in this study however, and a tilt angle to be select that when allows maximum solar radiation absorption all year. For comparison with other angles of inclination this angle must be used as the reference angle. A solar collector is to be inclined to the latitude of a location at an angle equal to maximum annual solar radiation absorption. Angle of reference for solar chimney mounted on roof was therefore 34° , representing the latitude of Jodhpur India.

3.4.1.4 *Dimensions of various solar chimney components*

Thermal performance gap of solar chimneys defines that, between the air gap of absorber wall and solar chimney was varied between 0.15 and 0.75 m. As reference, a 0.25m air gap was selected.

Roof and wall solar chimneys have the same size wall and glass cover. As explained earlier, the solar chimneys were reference length & width of 2m & 1m. Height of chimney was between 0.5m and 3m (equivalent to the wall of the absorbers and the glass cover). Glass covers generally 4 mm in thickness and 0.1 m in thickness for insulation walls. It was also expected and stated the following solar chimney area entrance covering the solar chimney base:

$$A_i = d \times W_{abs} \quad (3.18)$$

The outlet area should have been the same as the entrance area, thus the outlet area should have been equal to A_0 . The design parameters for solar fireplaces on the walls and the references to the roofs are shown in Table 3.3. Different design parameters have been studied in Table 3.4 for this study.

Table 3.3: For reference situations, design parameters for solar chimney [18]

Design parameter	Wall Solar Chimney	Roof Solar Chimney
Orientation	South Facing	South Facing
Angle of Inclination	Vertical (90°)	35°
Absorber wall dimension	2 m × 1 m	2 m × 1 m
Glass cover dimension	2 m × 1 m	2 m × 1 m
Glass cover thickness	4 mm	4 mm
Wall insulation thickness	0.1 m	0.1 m
Air gap	0.25 m	0.25 m
Ratio of outlet area to inlet area	1	1
Dimension of room to be ventilated	3 m × 3 m × 3 m	3 m × 3 m × 3 m

Table 3.4: Parameter Investigated in this study [12]

Parameter of Design	Wall Solar Chimney		Roof Solar Chimney	
	Design Value	Range Studied	Design Value	Range Studied
Angle of inclination	90°	90°	35°	32° to 74°
Air gap	0.24 m	0.16 m to 0.74 m	0.24 m	0.16 m to 0.74 m
Height of Chimney	1 m	0.6 m to 3 m	1 m	0.6 m to 3 m

3.5 Mathematical Models

CFD have been used to numerically solve the solar chimney performance. The following programmers are currently being used. Furthermore, used CFD modelling techniques in computer software for numerical research on solar chimneys.

The thermal efficiency of several solar chimney designs was evaluated using the CFD Program. CFD is a programming language of greatest interest in the performance of science and engineering calculations.

The energy balance on three components, the glass cover, absorber wall, & air inside duct, were examined in order to develop a mathematical model of a solar chimney. It was also calculating air stream mass balance. It is important to emphasize the assumptions made in this study before setting up energy and mass balance.

3.5.1 Assumptions

For this study the following expectations have been made:

- a) The steady-state have been adopted for the entire system.
- b) For heat transfer processes throughout the system, heat transfer assumed one dimension.
- c) The air temperature should be equivalent to ambient temperature at solar chimney entrance, namely $T_{fi}=T_i=T_a$, as well.

3.5.2 Energy balance equations

For the wall mounted solar chimneys and the roof mounted same mathematical model applies. The total thermal grid for the solar chimneys. Solar radiation touches glass cover surface and is passed to the wall absorber. The top of glass cover loses heat to the environment, while insulated absorber wall loses heat to the adjacent room. Radiation from absorber wall & convection from its glass cover transfer heat. The airflow and from absorber wall to cover of airflow. In view of the above-mentioned assumptions and thermal flow processes through the solar chimneys, the energy balance equation has been generated.

3.5.3 Glass cover with Energy Balance

Thermal flow into glazed cover consists of total of two apparatuses, namely heat of sunlight and heat from absorber wall; while flow of heat into surrounding dust is conclusion of air loss from sun and to glass cover, the heat flows.

The glass cover energy balance may thus be determined by:

$$S_1 \times A_g + h_{rwg} \times A_g \times (T_w - T_g) = h_g \times A_g (T_g - T_f) + U_t \times A_g (T_g - T_a) \quad (3.19)$$

3.5.4 Energy Balance on absorber wall

Solar radiation is responsible for the transfer of heat from a glass cover to absorber wall. Thermal flow from flexible wall consisting responsibility to identify three essentials: convective heat in air movement, radiative heat in glass cover heat in adjacent room.

On the absorber's wall, the energy balance might be:

$$S_2 \times A_w = h_w \times A_w \times (T_w - T_f) + h_{rwg} \times A_w (T_w - T_g) + U_b \times A_w (T_w - T_r) \quad (3.20)$$

3.5.5 Air flow Energy balance

The heat emitted by the air flow (q) is total thermal heat in the glass panel, and the convective heat in absorbing wall. The heat the solar chimney receives from the air.

The heat flow equilibrium between the absorber wall & glass cover must be determined:

$$q = h_w A_w (T_w - T_f) + h_g A_g (T_g - T_f) \quad (3.21)$$

The heat that was transmitted to the air flow:

$$q = m_{cf1} (T_{f,o} - T_{f,i}) \quad (3.22)$$

The solar chimney entering temperature is considered to be same to the room temperature. In evaluating average temperature of air in flow of air, following correlation is performed.

$$T_f = \gamma_{MTA} \times T_f + (1 - \gamma_{MTA}) \quad (3.23)$$

A value of 0.75 was found for the constant γ_{MTA} experimentally determined the value of γ_{MTA} and 0.74. In this investigation, the value for the constant is 0.74, as was usually used in earlier studies on solar chimney.

From Equation (3.23) & $T_{f,o}$ the formula and assuming $T_{f,i} = T_r$ the following equation is:

$$T_{f,o} = [T_f - (1 - \gamma_{MTA})] \gamma_{MTA} \quad (3.24)$$

The following equation may be derived by inserting equation (3.24) into equation (3.22):

$$q = m_{cf1} [T_f - T_r] \gamma_{MTA} \quad (3.25)$$

The following equation is obtained by substituting equation (3.25) into equation (3.21):

$$[-m_{cf1} T_r] \gamma_{MTA} = h_w A_w T_w + h_g A_g T_g - T_f [m_{cf} \gamma_{MTA} + h_w A_w + h_g A_g] \quad (3.26)$$

The following set of three equations may be obtained by rearranging equations (3.19), (3.20), and (3.26) as follows:

$$(h_{rwg} A_w + h_g A_g + U_t \times A_g) T_g - (h_g A_g) - (h_{rwg} A_w) = S_1 A_g + U_t \times A_g \times T_a \quad (3.27)$$

$$-h_{rwg} A_w T_g - h_w A_w T_f + (h_w A_w + h_{rwg} A_w + U_b A_w) = S_2 A_w + U_b A_w T_r \quad (3.28)$$

$$h_g A_g T_g - \left[h_g A_g + h_w A_w + \frac{m_{cf1}}{\gamma_{MTA}} \right] T_f + h_w A_w T_w = - \left(\frac{1}{\gamma_{MTA}} \right) T_r \quad (3.29)$$

3.5.6 Balance of Mass

The following formula may be used to determine the mass flow of air in a solar chimney:

$$m = C_d \times \rho_{f1} \times A_{out} \sqrt{\frac{2g L \sin \beta (T_f - T_r)}{(1 + A_r^2) T_r}} \quad (3.30)$$

$$A_r = \frac{A_{out}}{A_{in}} \quad (3.31)$$

To determine the temperatures of the glass cover, absorber wall, and air flow, as well as the mass flow rate, above equations (3.27), (3.28), (3.29) and (3.30) have been used. The procedure for doing this is described below. The step-by-step procedure.

3.6 Solution Procedure

The mathematical model produced in this study was solved with the help of a CFD program. The following is a step-by-step guide to accomplishing this.

3.6.1 Astronomical parameters

In CFD, Indian geographical co-ordinates were entered. However, latitude has been assigned a positive value, because India is in Northern Hemisphere, a place north of equator has a positive value, consisting south of equator has a negative value.

The standard meridian local time zone was calculated as follows:

$$L_{standard} = \text{Time difference between Indian time and GM time} \times 15 = 5.5 \times 15 = 80.5^\circ \quad (3.32)$$

The decline angle, solar time, the angle of the hour, the angle of sunset and solar zenith was determined using the formulae. The angle of azimuth on the north face is 180° while in the Northern Hemisphere the angle of azimuth on the surface is 180° . As such, this research assumed that the azimuth angle of the surface was 180 degrees, with India in the northern hemisphere & solar chimneys in the south.

An equation then was used to calculate the beam incidence angle on a surface. A surface albedo is 0.2 when the average temperature for the year is above 0°C & 0.7 when annual temperature is below -5°C . The temperature data were analyzed and the annual temperature was determined to be higher than 0°C & As a result, the albedo was given a value of 0.2.

3.6.2 Attenuation & Radiation of Solar

On a sloped surface, total radiation of solar was estimated using formulae to calculate different astronomical parameters. The transmission, reflection and absorption of the glass cover were estimated using formulae.

In the case of a transparent medium, part of this radiation is reflected, some is absorbed, but some of it is also transmitted. The reflected portion of radiation is referred to as reflection (ρ), the absorbed fraction is defined as absorption (α) and the transmitted fraction is referred to as transfer (τ) and sums of these three parts are referred to as given equations.

$$\alpha + \tau + \rho = 1 \quad (3.33)$$

The perpendicular radiation components of a single cover are determined to be the transmittance, absorption and reflection associated with them, as used: The following equations are available:

$$\tau_{perpendicular} = \tau_a \times \frac{(1 - r_{perpendicular})^2}{(1 - (r_{perpendicular} \times \tau_a))^2} \quad (3.34)$$

$$\alpha_{perpendicular} = (1 - \tau_a) * \frac{(1 - r_{perpendicular})}{(1 - r_{perpendicular} \times \tau_a)} \quad (3.35)$$

$$\rho_{perpendicular} = 1 - (\alpha_{perpendicular} + \tau_{perpendicular}) \quad (3.36)$$

The transmittance, absorption, and reflection of the parallel component of radiation may all be calculated using the same formulae.

$$\tau_{parallel} = \frac{\tau_a \times (1 - r_{parallel})^2}{(1 - (r_{parallel} \times \tau_a))^2} \quad (3.37)$$

$$\alpha_{parallel} = \frac{\{(1 - \tau_a) \times (1 - r_{parallel})\}}{(1 - r_{parallel} \times \tau_a)} \quad (3.38)$$

$$\rho_{parallel} = 1 - (\tau_{parallel} + \alpha_{parallel}) \quad (3.39)$$

$$\tau_a = \exp \exp \left(-\frac{K_{eczglass}}{\cos \cos \theta_2} \right) \quad (3.40)$$

$$\theta_2 = n_1 \times \sin \sin \theta_1 \} / n_2 \quad (3.42)$$

$$r_{perpendicular} = \frac{\sin^2(\theta_2 - \theta_1)}{\sin^2(\theta_2 + \theta_1)} \quad (3.43)$$

$$r_{parallel} = \frac{\tan^2(\theta_2 - \theta_1)}{\tan^2(\theta_2 + \theta_1)} \quad (3.44)$$

Then, averaging the transmission of the single cover for perpendicular and parallel radiation components can be calculated. The same method can be used for the calculation of absorption and cover reflectivity.

$$\tau = \left(\frac{1}{2}\right) \times (\tau_{perpendicular} + \tau_{parallel}) \quad (3.45)$$

$$\alpha = \left(\frac{1}{2}\right) \times (\alpha_{perpendicular} + \alpha_{parallel}) \quad (3.46)$$

$$\rho = \left(\frac{1}{2}\right) \times (\rho_{perpendicular} + \rho_{parallel}) \quad (3.47)$$

Air and glass refractive indices, n_1 and n_2 , were allocated in equation, respectively 1 and 1.526. In addition, K in equation was given a mean value of the extinction coefficient of 18 m^{-1} , since K varies from 4 m^{-1} until 32 m^{-1} in different kinds of glass. A medium's refractive index is a property that includes the absorption, emission, and dispersion effects of its molecules.

In the following calculations were made, the solar radiation quantity absorbed into the absorber wall & glass cover referred to in S_1 and S_2 :

$$S_1 = \alpha \times I_t \quad (3.48)$$

$$S_2 = \alpha_{wall} \times \tau \times I_t \quad (3.49)$$

The values were calculated using equations (3.27) and (3.28) for the transfer (α) and the absorption of the glass coverage. As was used in previous studies on solar chimneys, the absorbent wall (α_{wall}) was supported by 0.95.

3.6.3 Components of the solar chimney's temperature

The next step was to calculate the fluid (Glass cover, air stream & absorber wall) which were respectively signified by T_f , T_g and T_w . To that purpose, the convective heat transfer coefficient and other physical properties of air were determined. It was also essential, as these have no fixed values, to develop density correlations, specific thermal capacity, dynamic viscosity & thermal conductivity; depending on temperature, the values had to be calculated hourly throughout entire year

Temperatures ranging from 250 K to 1000 K were used to compute density, heat capacity, dynamic viscosity, and thermal conductivity. The connections were created in a table for Excel. To fit the data on a curve, a graph was created and a trend line was used for each physical feature. During period, the determining coefficient was 1 to guarantee the best fit, commonly known as R-squared value. In order to adapt this data to the curves, polynomial lines of orders 2, 3, 4 and 5 were created.

Annex "A" contains the density, specific temperature capacity, dynamic viscosity, & thermal conductivity correspondences, as well as formulae needed to determine the kinetic viscosity of air.

For every component of the solar chimney, the mean monthly temperatures were calculated according to the following:

$$n = \text{number of days in each month} \times \text{number of hours in 1 day} \quad (3.50)$$

Where, T_i shows instantaneous wall, glass covering, flowing and ambient air temperature (T_w , T_g , T_f & T_a); Each month's data points are represented by n & T_{iavg} is the

monthly mean absorber wall temperatures, glass coverage, fluid, & ambient air ($T_{w,ave}$, $T_{g,ave}$, $T_{f,ave}$ & $T_{a,ave}$).

It is important to note that at each data point, two values were calculated in order to take into account that air stream, namely absorber wall & glass cover, are surrounded by various bounders. The existing literature equations were used to calculate other physical features.

3.6.4 Correlations of convective heat transfer

Aside from physical characteristics of air, the following are all equations utilized in the simulation of the CFD, heat transfer correlations were essential for calculating the air cover temperature, absorber wall and air stream.

3.6.4.1 Prandtl Number

This is a dynamic viscosity, specific thermal capacity and thermal conductivity, is a dimensional constant. It is possible to state the following: -

For glass cover & air stream,

$$Pr = \frac{\mu_f \times C_f}{K_f} \quad (3.51)$$

For absorber wall & air stream,

$$Pr_1 = \frac{(\mu_{f1} \times C_{f1})}{K_{f1}} \quad (3.52)$$

3.6.4.2 Grashof Number

The ratio of buoyant to viscous forces is known as the Grashof number.

For glass cover & air stream,

$$Gr = \frac{(g \times \beta \times \Delta T \times L_{stack}^3)}{v_f^2} \quad (3.5)$$

$$\beta = \frac{1}{T_m} \quad (3.54)$$

$$\Delta T = T_g - T_f \quad (3.55)$$

For inclined solar chimneys:

$$L_{stack} = L_{abs} \times \sin \beta \quad (3.56)$$

For wall-mounted solar chimneys:

$$L_{stack} = L_{abs} + \left(\frac{z}{2}\right) \quad (3.57)$$

For absorber wall and air stream,

$$Gr_1 = \frac{(g \times \beta_1 \times \Delta T_1 \times L_{stack}^3)}{v_{f1}^2} \quad (3.58)$$

$$\beta_1 = \frac{1}{T_{m1}} \quad (3.59)$$

$$\Delta T_1 = T_w - T_f \quad (3.60)$$

3.6.4.3 *Rayleigh Number*

The product of the Prandtl and Grashof numbers equals the Rayleigh number.

For Air stream & Glass Cover,

$$R_r = G_r \times P_r \quad (3.61)$$

For air stream and absorber wall,

$$R_{r1} = G_{r1} \times P_{r1} \quad (3.62)$$

3.6.4.4 *Nusselt Number*

The Rayleigh and Prandtl numbers are used to calculate Nusselt number, as shown in formulae below:

For air stream and glass cover,

State 1- for $R_a < 10^9$,

$$N_{uf} = 0.68 + \left\{ \frac{0.670 \times Ra^{\frac{1}{4}}}{\left[1 + \left(\frac{0.492}{Pr} \right)^{\frac{9}{16}} \right]^{\frac{4}{9}}} \right\} \quad (3.63)$$

State 2: for $10^{-1} < Ra < 10^{12}$,

$$N_{uf} = 0.825 + \left\{ \frac{0.387 \times Ra^{\frac{1}{6}}}{\left[1 + \left(\frac{0.492}{Pr} \right)^{\frac{9}{16}} \right]^{\frac{8}{27}}} \right\} \quad (3.64)$$

For air stream & absorber wall,

State 1: for $Ra < 10^9$,

$$N_{uf} = 0.68 + \left\{ \frac{0.670 \times Ra_1^{\frac{1}{4}}}{\left[1 + \left(\frac{0.492}{Pr_1} \right)^{\frac{9}{16}} \right]^{\frac{4}{9}}} \right\} \quad (3.65)$$

State 2: for $10^{-1} < Ra < 10^{12}$,

$$N_{uf} = 0.825 + \left\{ \frac{0.387 \times Ra_1^{\frac{1}{6}}}{\left[1 + \left(\frac{0.492}{Pr_1} \right)^{\frac{9}{16}} \right]^{\frac{8}{27}}} \right\} \quad (3.66)$$

The equations (3.63) to (3.64) were also mentioned, that means the minimum inclination angle with horizontal must be at 30° , for plane sides that are inclined to a 60% or greater angle with the vertical. The minimum horizontal tilt angle for the solar chimney on the roof was 30° in this study and equations (3.63-3.66) could therefore be applied.

3.6.5 Coefficients of Heat transfer

In addition, the varied coefficients of heat transfer in the equations that reflect solar chimney system energy balancing equations must be calculated.

3.6.5.1 *The solar radiation transfer coefficient between the wall and the glass.*

Between the glass cover & absorber wall, the coefficient of radiative heat transfer was estimated as follows:

$$hrwg = \frac{\sigma \times (T_g^2 + T_s^2)(T_g + T_s)}{(1/\epsilon_g + 1/\epsilon_w - 1)} \quad (3.67)$$

The ϵ_g and ϵ_w signs are referred to in the studies the absorber wall and glass cover emissivity, each time, 0.9 & 0.95 are considered to represent the values. The Stefan Boltzmann Constant (σ) is $5.67 \times 10^{-8} \text{ W}\cdot\text{m}^{-2}\cdot\text{K}^{-4}$

Since this research also examines the view factor effect on solar chimneys, the radiative coefficient of heating transfer between the absorber wall & glass cover should be measured view factor between the two components into consideration. The following formula was used to get the heat transfer coefficient:

$$h_{rwg} = \frac{(T_g^2 + T_s^2)(T_g + T_s)}{\left\{ \frac{1 - \epsilon_w}{\epsilon_w} \right\} + \left\{ \frac{1 - \epsilon_g}{\epsilon_g \times A_g} \right\} \times A_{abs} + \frac{1}{F_{w-g}}} \quad (3.68)$$

3.6.5.2 *Convective heat transfer coefficient between air-glass and air-wall*

From following equations: It is possible to compute the coefficient of convective heat transfer h_g between air stream & glass cover, including coefficient of the convective thermal transfer h_w between the air stream and absorber wall:

$$h_g = \frac{Nu \times K_f}{L_g} \quad (3.69)$$

$$hw = \frac{Nu1 \ kf1}{Labs} \quad (3.70)$$

3.6.5.3 *Coefficient of heat transfer between absorber wall & adjacent room*

The total heat transfer coefficient between the wall absorber insolation & the air gap that must be ventilated as following equation

$$U_b = \frac{K_{ins}}{W_{ins}} \quad (3.71)$$

Polyurethane with a thermal conductivity $0.027 \text{ Wm}^{-1}\text{K}^{-1}$ at room temperature was the insulation material under study.

3.6.5.4 Coefficient of total heat transfer of the glass cover top

The major cause of heat is the radiation from the cover of the glass to the clouds and convection from top of glass panel by wind. Total thermal transfer loss coefficient can so be as described in the following equation

$$U_t = h_{rs} + h_{wind} \quad (3.72)$$

The equation below gives radiative heat transfer coefficient between glass cover and spiritual.

$$h_{rs} = \sigma \times \epsilon_g (T_g^2 + T_s^2)(T_g + T_s) \quad (3.73)$$

Correlation calculates the coefficient for thermal convection by wind:

For $V \leq 5 \text{ m/s}$,

$$h_{wind} = 3V + 2.8 \quad (3.74)$$

For $V > 5 \text{ m/s}$,

$$h_{wind} = 6.15 \times V^{0.8} \quad (2.75)$$

CHAPTER 4

4. RESULTS & DISCUSSION

The performance is modelled using CFD for many solar chimney constructions and the rate of change each hour. Chapter 2 covered initial research on solar chimneys & different performance characteristics of solar chimneys in Chapter 3, including solar radiation energy, air, and chimney height and tilting angles and glazing types. The influence of view factor was typically covered in previous solar chimney research. In this study, effect on thermal efficiency was studied of wall and roof mounted solar panels, air gap, and altitude or chimney height. The model validation & CFD simulation results and the analysis of results are provided in the current chapter.

4.1 Results of Climate data

There are two primary climatic elements in the solar chimney performance: wind speed & solar radiation intensity. The intensity of solar radiation, is the driving factor behind the solar chimney's effectiveness. It has already been indicated that a larger number of sun rays raises the air temperature in the solar chimney, resulting in a higher stack pressure. Previous studies of solar panels have shown that with the sun's intensity, the venting rate rises. The ambient temperature is also a crucial climate parameter for estimating solar chimney performance and is closely connected to atmospheric temperature and solar radiation intensities.

The wind is the second most common climate variable that affects solar chimney performance by either improving the airflow in solar chimney or by preventing it. When the low airflow rate was at the least wind speed and the highest airflow rate was obtained, experimental research on solar chimney was performed.

For this research, climate data includes the level of solar radiation, temperature & wind speed. Given data collected used for the study was available monthly, which involved 8760 from 365 days, multiple of 24 hours. The following information was gathered:

- On a horizontal surface, diffusion radiation & global radiation intensities are given in $\frac{W_h}{m^2}$,
- Velocity of the wind, in m/s.

- Temperature at °C.

The weather information was collected from the Indian Solar Radiation Database, and it says that the quality of this meteorological data collection is good. Figures 4.1 and 4.2 illustrate the climatic data consistent with the research. Each month, the hourly results were aggregated for each climatic parameter, which gave a monthly average to illustrate the basic sets of data.

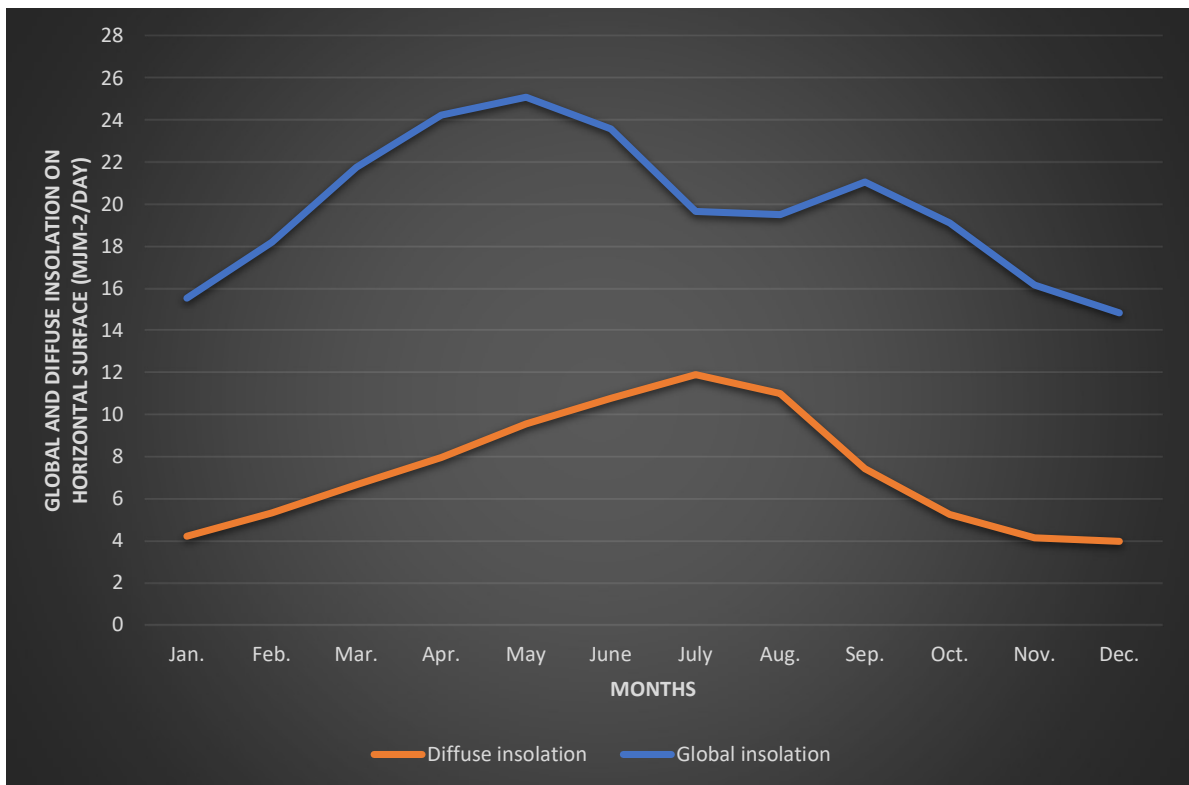


Figure 4.1: Monthly average global (I_g) & diffuse insolation (I_d) given in India on a horizontal surface.

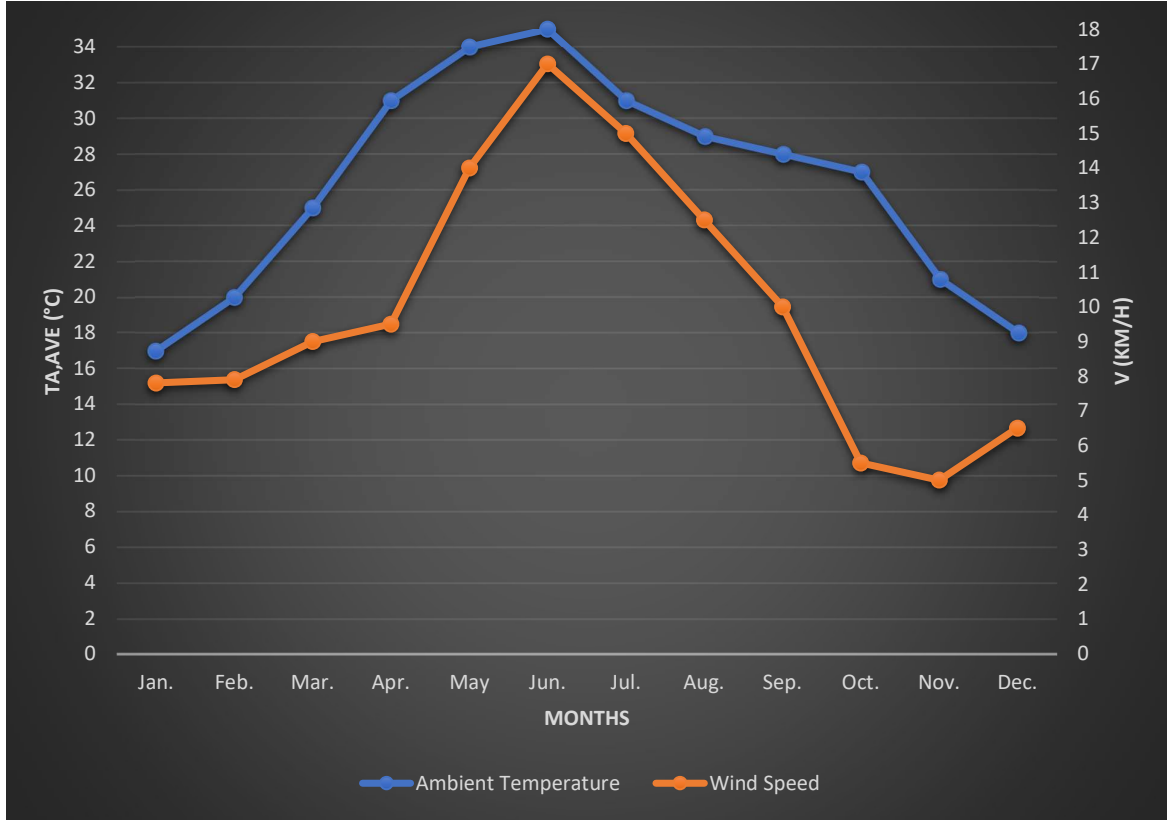


Figure 4.2: Monthly average ambient air temperature & wind speed in Jodhpur India.

4.2 Simulation in CFD

Three equations have been found for three unknown temperatures after the development of the different correlation between the air properties and the calculation of coefficient of all heat transfer (T_f , T_g and T_w). In order to write if for T_g and T_w , equation (3.12) has been rearranged. Equations have also been redesigned for T_g and T_w , as shown by the following equations, to be the subject of formulation, respectively:

$$T_f = h_g A_g T_g + h_w A_w T_w + \frac{(m_{cf1} \times \frac{T_r}{YMTA})}{(h_g A_g T_g + h_w A_w T_w + \frac{m_{cf1}}{YMTA})} \quad (3.1)$$

$$T_g = \frac{(S_1 A_g + U_t A_g T_a + h_g A_g T_f + h_{rwg} A_w T_w)}{(h_g A_g + h_{rwg} + U_t A_g)} \quad (3.2)$$

$$T_w = \frac{(S_2 A_w + U_b A_w T_r + h_{rwg} A_w T_g + h_w A_w)}{(h_w A_w + h_{rwg} A_w + U_b A_w)} \quad (3.3)$$

The equations were then solved in CFD together, which consisted of a series of linear simultaneous equations. Two methods can be employed, namely direct & iterative methods, for solving certain linear simultaneous equations. Examples of direct techniques are Gaussian elimination procedures, decomposition of LU, and the Cramer rule, whereas approximate solutions include Jacobi method, Gauss-Seidel method & following combination.

The iterative approach for addressing unknown materials was used in this study since the fluid characteristics and coefficients for transfer of heat are dependent on temperature. A method of iterative to characterize as one is repeated performed from the first step to the second step, etc. The Gauss-Seidel iterative technique has been employed in this research as it is the most often used iterative method and also offers effective corporate governance, as fresh estimations are made accessible to the arithmetic process.

The process used for solving the many equations associated with the solar chimney performance in CFD is illustrated in the figures. Firstly, all constants and design parameters for CFD solar chimneys had to be entered. For fluid, glass and absorber walls, the starting temperatures were determined. All essential equations in CFD have been input and solved accordingly in an iterative procedure up to the resolution of the results.

4.2.1 Performance Evaluation of Solar Chimneys

A Solar Chimney performance commonly determines ventilation rate (V_{rate}), typically expressed in m^3/s and as follows:

$$V_{rate} = \frac{m}{\rho_{f1}} \quad (3.4)$$

The parameter used in several studies for assessing the solar chimney performance is ACH. The ventilation rate is typically expressed in ACH by another means. An important analytical parameter ACH, it is standard ventilation in many others countries be available.

For example, 3 ACH is the minimum in line with the standard ventilation needed for residential structures in India. For meeting rooms, kitchens, meeting rooms, or health-related areas, the minimum HCA requirement is significantly higher, ranging from 6 to 20. In India, amenities in hotel offices and lobbies should be at a level of at least 2 ACH,

including educational buildings and conference rooms. For computation of ACH, the following equation is used:

$$ACH = \frac{V_{rate} \times 3600}{V_{room}} \quad (3.5)$$

The volume of the ventilation chamber was estimated as follows:

$$V_{room} = L_r \times W_r \times H_r \quad (3.6)$$

During the investigation, a ventilation rate indicator, the solar chemist's performance was based on the evaluation of ACH. The effects of air space, incline angle, chimney height & view factor were investigated by the side of ACH. In order to record the ACH values by air changing each hour every month, the total ACH is calculated monthly in an average form. Every month, the amount of time is divided.

4.2.2 Analysis of statistic

The conclusions of the simulation in this experiment are analogous to the conventional values produced to validate the mathematical model. The same design parameters as those used during CFD research are used in the mathematical model for use in this study to determine solar chimney performance. The Mathur, Mathur and Anumpa (2006) numerical & experimental research on inclined solar chimney without taking the view factor into account. Since results of solar panels were included in this study, with & without view factor, numerical numbers were compared with literature, with or without view factors, for each of these situations.

In order to achieve solar radiation intensity ranging from 500W/m², for a 1m high & width absorber, the air gap was examined at 45° inclined at various ambient temperatures for performance of an inclined solar chimney (as regards exit air flow speed). Moreover, 0.037 W/(m-K) was assumed to be the thermal conductivity of insulation material & 0 speed of wind was expected to be applicable to the same parameters Mathur, Mathur, and Anumpa used for (2006)". The airflow rate at departure was calculated as follows:

$$V_o = \frac{m}{\rho_{f1} \times A_{out}} \quad (3.7)$$

The percentage deviation root mean square e_i was calculated as follows:

$$e_i = \left\{ \frac{X_i - Y_i}{X_i} \right\} \times 100 \quad (3.8)$$

"If X_i denotes the value obtained from this numerical simulation then, Y_i denotes the testing value obtained.

4.2.3 Solar radiation incident on sloping and vertical surfaces

CFD software has estimated solar radiation on painted surfaces at a 34° angle (free speed, direct and ground reflection). The solar radiation incidents on these surfaces need to be computed since the data supplied gives global, diffuse solar radiation in a horizontal region. For printable graphs, computed values are sent to Excel. The hours of the solar radiation incident were estimated at an average monthly rate of one month across the whole year.

Following Fig.4.3, in June, the maximum solar radiation value incidence on both surfaces was achieved, while in January it was the least. In addition, incidents of solar radiation in October-March were lower than in April-September. Because winter is between October and March, the northern hemisphere tilts towards the sun throughout the months of April and September, with the seasonal changes in sunshine as the earth rotates and is at a 23.5° angle slanted towards the orbital plane.

Furthermore, the incident solar radiation in comparison with the vertical surface throughout the year is significantly higher on the inclined surface. For the inclined and vertical surfaces, the highest amounts of solar power were 1.05 MJ/m²/hour and 0.35 MJ/m²/hour for June, respectively, according to Figure 4.3. As a result, the amount of solar energy incident on the sloping surface was over three times higher. This means the amount of radiation gathered on a surface reduces as the angle of inclination increases. The solar collector tilt angle is the angle that makes it possible for sunlight to perpendicularly impact the surface. Therefore, solar radiation is significantly higher on the sloping surface as it allows the sunlight to surface at an angle of less than 90° near the surface of vertical.



Figure 4.3: Average monthly incident insolation on inclined & vertical surfaces (I_t) in the Jodhpur, India.

In addition, if the angle of the photograph is approximately equivalent to the latitude of the position, the camera is able to capture maximum solar radiation from the solar collector. The amount of solar radiation incident (with tilt angles of 34°) on a slanted surface is therefore greater than on a vertical surface.

4.3 Validation of the Model

Table 4.1 provides a comparison of the experimental data from Mathur, Mathur, and Anupma (2006) with the model values from this work. For Model 1 (view factor) and Model 2, the errors were 13% and 20% respectively (view factor not visible). The outcomes of this investigation may thus be considered to be in accordance with the literature results. Furthermore, the integration of the visual component increases the precise solar chimney modelling by about 7 percent.

Table 4.1: Comparison of Mathur, Mathur and Anupma experimental results from 2006 with numerical results for the inclined solar chimney (45°)

derived from the model in this study. The View Factor is included in Model 1 but not in Model 2.

S (W/m ²)	T _a (K)	<u>Exit air flow velocity</u> (m/s)		
		Experimental	Model 1	Model 2
500	300	0.17	0.160	0.152
550	303	0.18	0.166	0.157
600	305	0.19	0.172	0.162
650	311	0.20	0.178	0.167
700	311.3	0.21	0.183	0.172
750	312.9	0.22	0.189	0.177

4.4 System component temperatures

4.4.1 Temperatures of the glass cover, wall, fluid, & ambient air absorbent

The wall temperature absorber, its glass coverings, the fluid (a chimney air system between the absorber walls & glass covers) and outside ambient air were averaged every month in such a way to achieve a monthly average temperature for the individual components of the vertical & inclined solar chimney.

January was the coldest month of the year in India, while June was the warmest. The ambient temperature curve shown in figures 4.4 and 4.5 was the trough and peak in these two months. Figure 4.4 and Fig. 4.5 show that both the inclined and vertical solar chimney fall in order in the first place in wall absorber temperature, trailed by the fluid, glass cover and outside ambient temperatures. That was expected because the absorbent wall was designed as a black body that traps much higher temperatures than the glass cover.

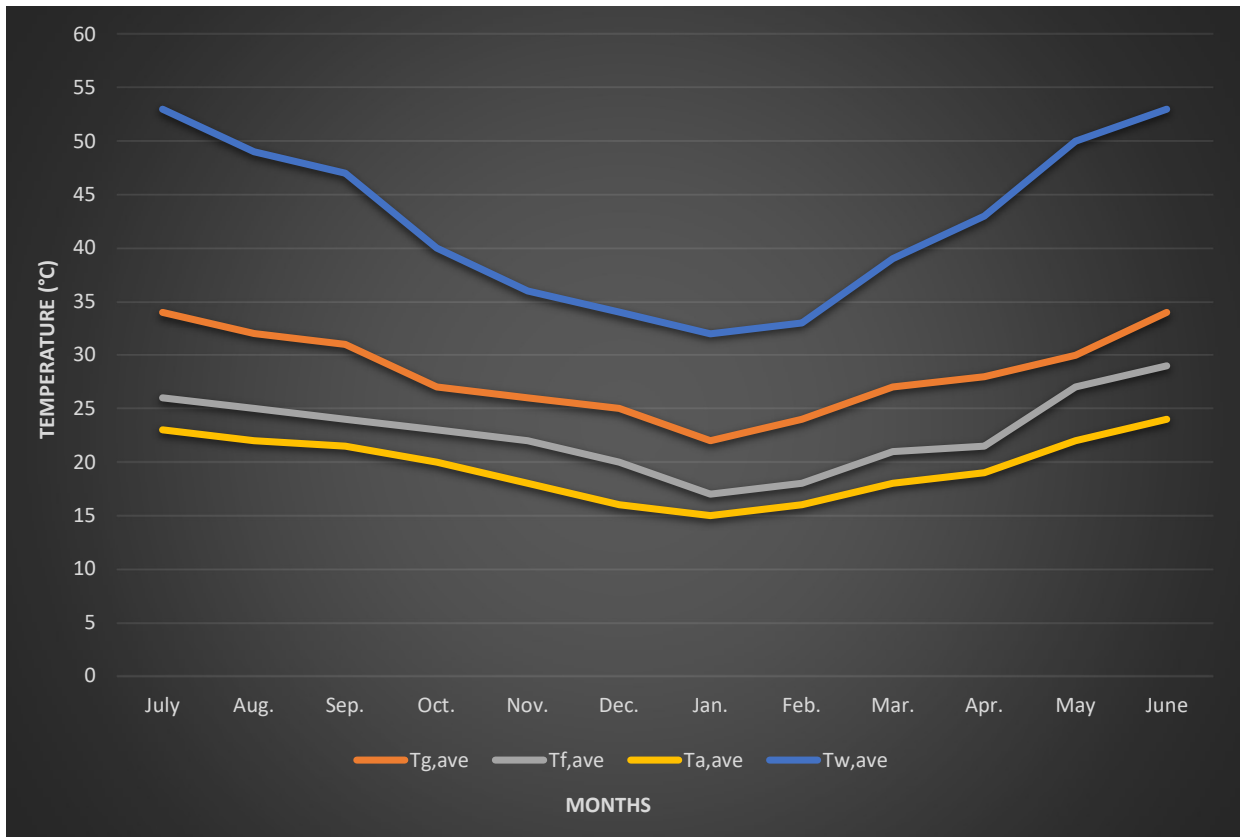


Figure 4.4: Average monthly temperatures are 34° to $d=0.25m$ and $L_{abs}=L_g=2m$ for absorber wall ($T_{w,ave}$), glass cover ($T_{G,ave}$), fluid ($T_{f,ave}$) and ambient air ($T_{a,ave}$) for the solar chimney in India.

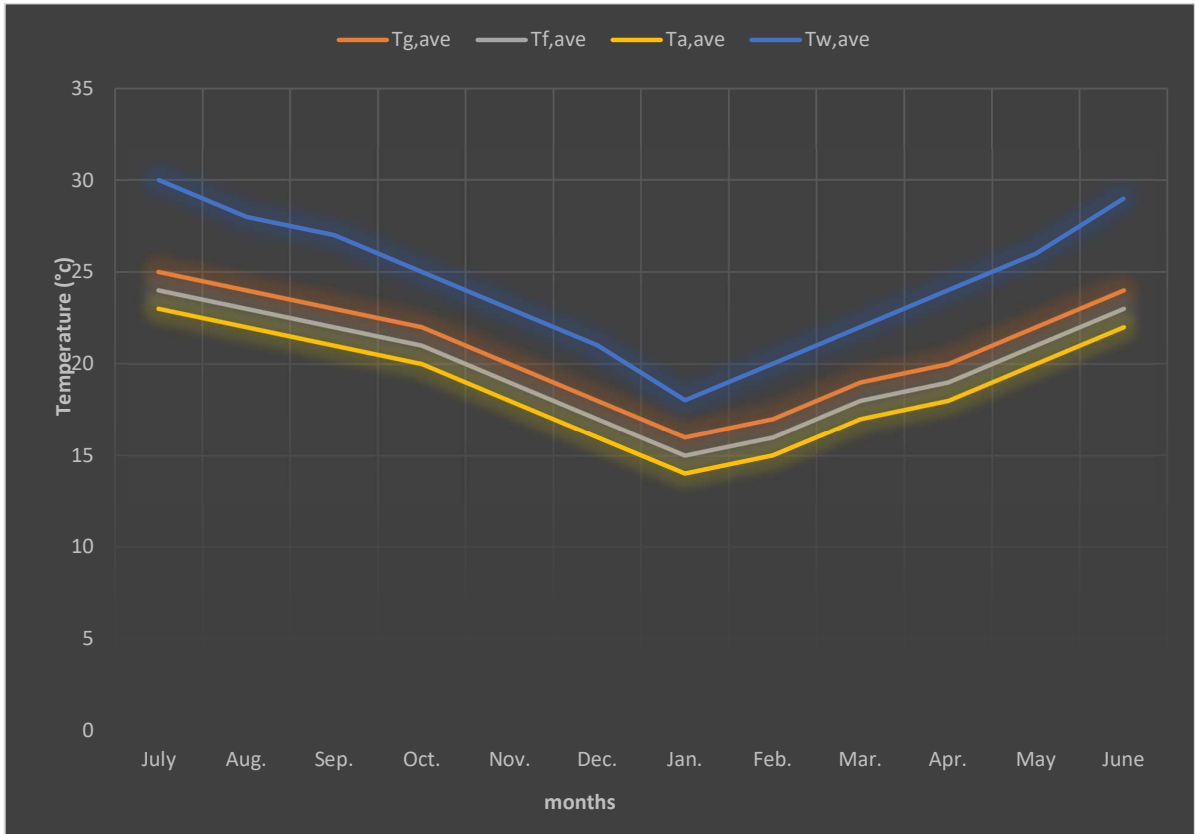


Figure 4.5: Average monthly temperature is Vertical to $d=0.25$ m and $L_{abs}=L_g=2$ m for absorber wall ($T_{w,ave}$), glass cover ($T_{G,ave}$), fluid ($T_{f,ave}$) and ambient air ($T_{a,ave}$) for the solar chimney in India.

The results of this study correspond to the results of previous studies. In an Ong (2003) numerical study, it was found that both the glass cover and the fluid are always tempered above the absorbers' wall. The wall absorber temperature is higher than the glass cover and the fluid due to radiation of thermal wall absorption was also established statistically.

Furthermore, fluid, glass and absorbent wall temperatures in both solar are greater in summer compared to winter. In summer, solar radiation intensity is greater and so the glass cover and the absorber wall may absorb additional energy and heat can be transmitted by convection to the flow of air. As a result, fluid, glass and absorber wall temperatures have risen as a result of the increase in solar radiation. The results of the research are

consistent with the results of previous research, which established that fluid, glass and wall temperatures increase when solar radiation intensity increases.

4.4.2 Comparison of inclined solar chimney temperatures with vertical solar chimney

Figures 4.6, 4.7, and 4.8 are compared with the fluid temperature, the glass cover temperatures, and the absorbers in the vertical & inclined solar chimney. Fig. 4.6 in Fig. 4.6, 4.7, and Fig. 4.8, the temperatures for the inclined solar chimney of all three sections (fluid, glass cover, and absorption wall) are above the respective vertical solar chimney component. The reason is that the solar radiation volume on a surface is decreasing as the angle of path rises, as indicated before. Furthermore, the maximum solar radiation from a solar chimney with a tilting angle equal to the location latitude has been studied. The 34-degree solar chimney may absorb more solar than the vertical solar chimney, resulting in greater glass, absorber wall, and fluid temperatures than the corresponding vertical solar chimney element.

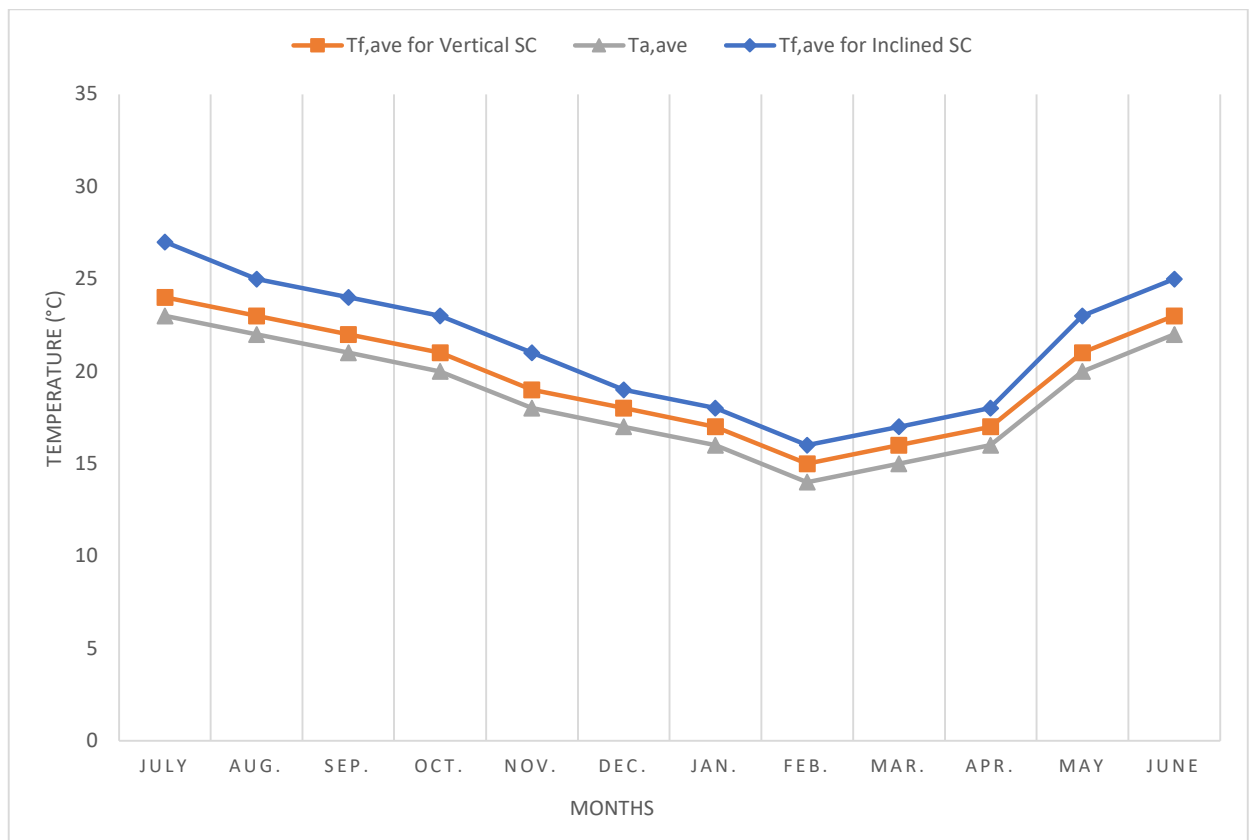


Figure 4.6: Average monthly fluid ($T_{f,ave}$) temperature for tilted solar panels with 34° inclined angles and vertical solar panels; $d=0.25$ m and $L_{abs}=L_g=2$ m in India.

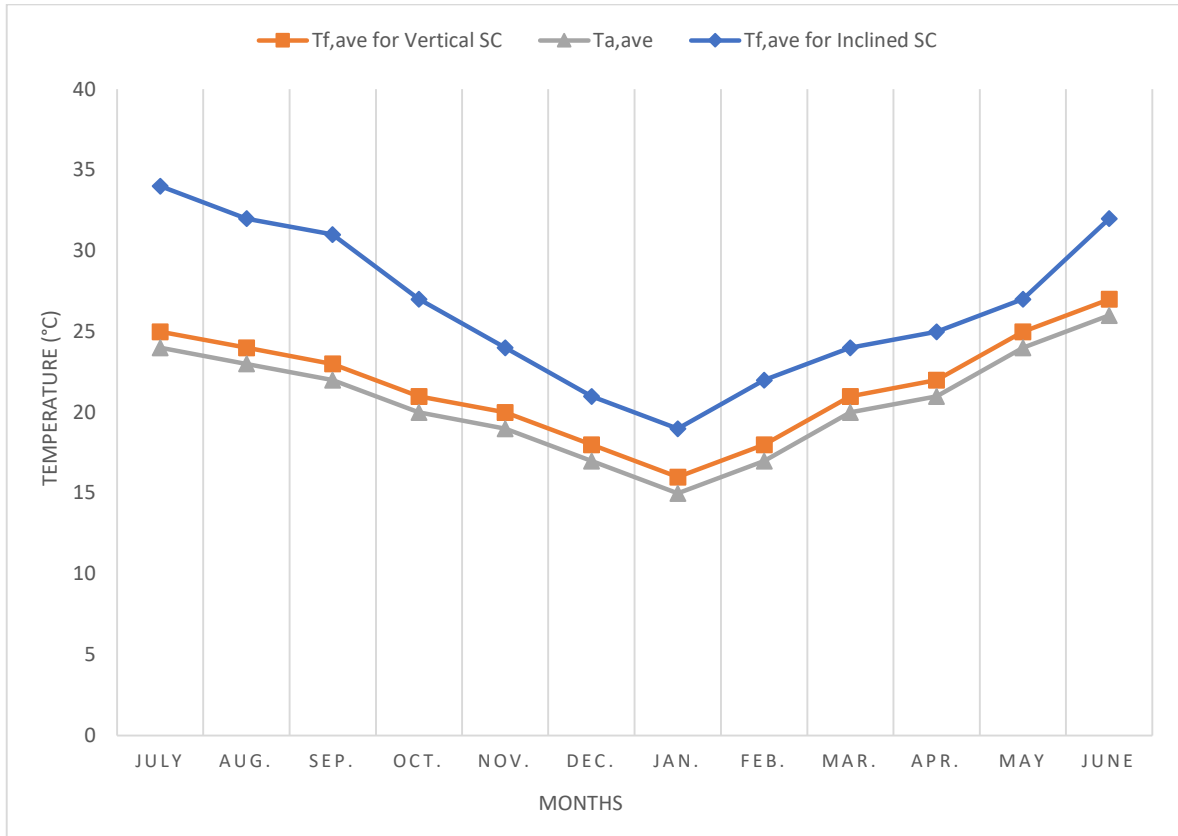


Figure 4.7: Temperatures of average monthly glass covered by a tilt angle of 34° and a vertical (90°) solar chimney ($T_{g,ave}$), $d=0.25$ m and $L_{abs}=L_g=2$ m in India.

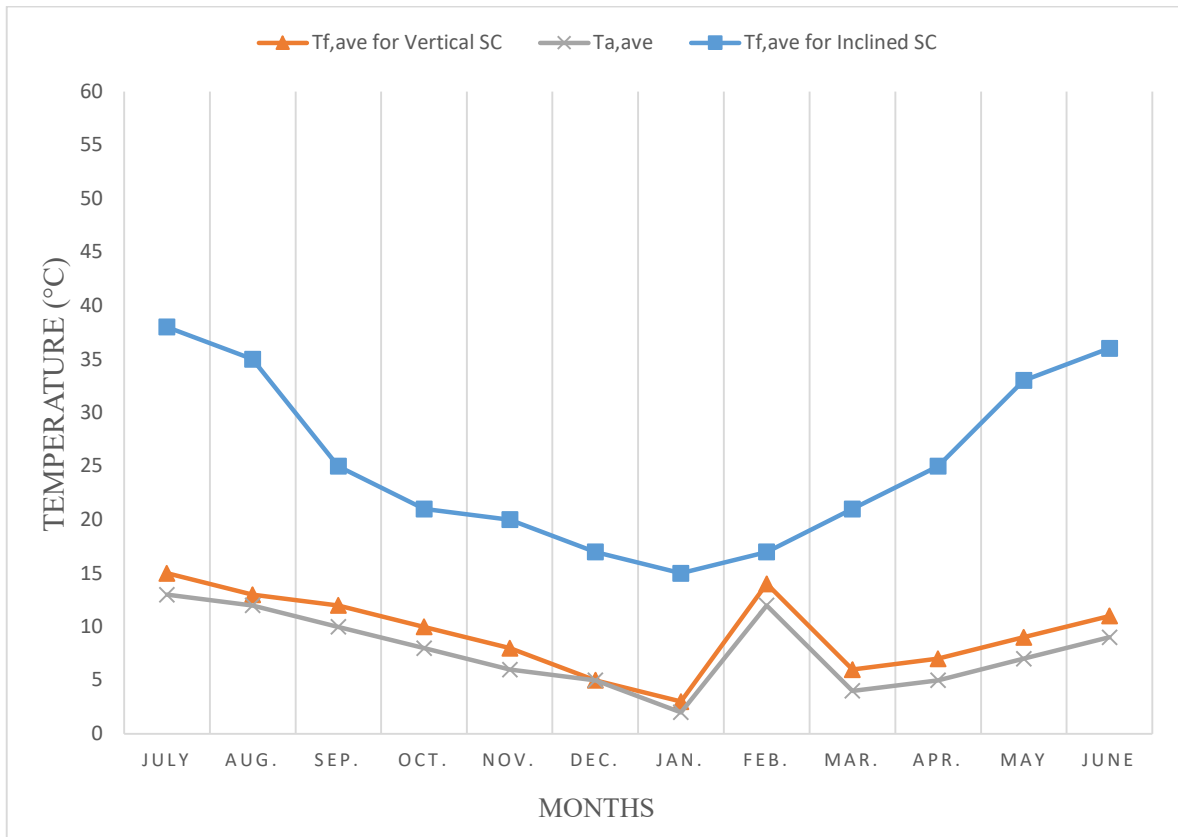


Figure 4.8: Average monthly wall temperature absorber T_w , ave for tilt-in solar chimney 34° tilt angle & vertical solar chimney with $d=0.25$ m and $L_{abs}=L_g=2$ m in India.

4.5 The impact of the inclination angle on the ACH

The Indian Weather Service reports that the seasons follow in India. From spring through February to April, and from summer May to August, and from autumn to October. This study shows the results for summer (May to August) and winter (November to January). As seen in figure 4.9, with an increased angle of inclination, the ACH changes from 30° to 60° , but with an additional rise in the angle of inclination, the ACH lowers. In winter as in summer, the highest angle is the 60° angle of inclination, The vertical solar chimney is the smallest in the winter and summer.

The highest ACH recorded in the month of February was 4.3 in the solar chimney, which is 60° inclined to the horizontal. During the summer season, the maximum ACH achieved was found to have an average value of 5.9 during July, a 60° inclination angle for

a solar chimney. The highest ACH was found at 4.3 for the vertical solar chimney, which was shown in Figure 4.7 during June. It is therefore possible to determine that, at 60° tilting, the inclined Solar Chimney can provide a higher ventilation rate of approximately 20% in the winter and summer than the vertical Solar Chimney.

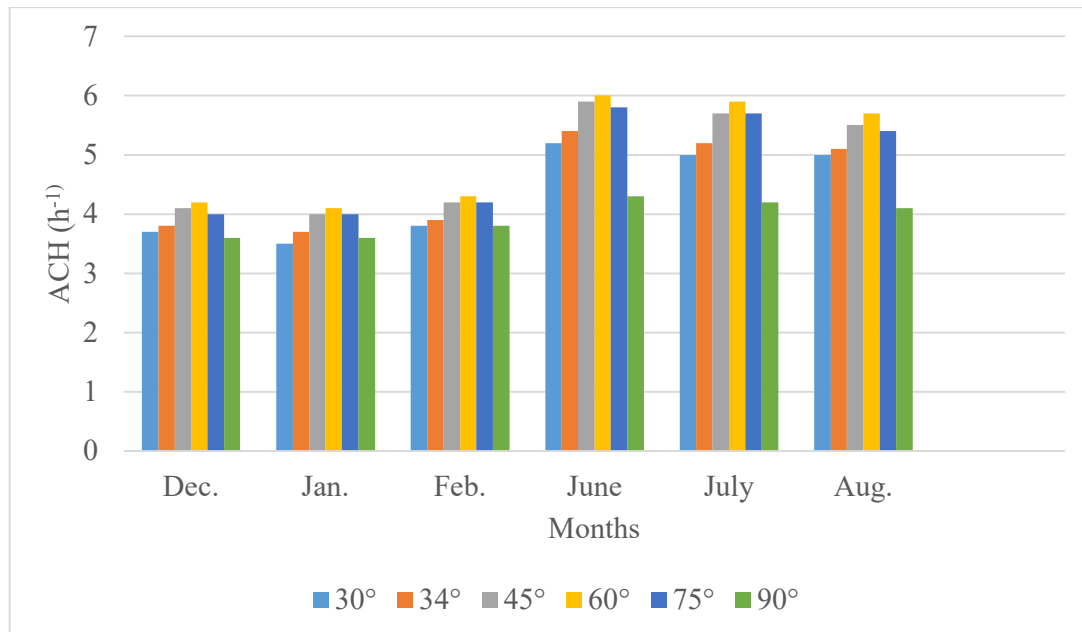


Figure 4.9: Inclination angle effect on average monthly ACH in winter & summer for inclined & vertical solar chimney with $d=0.25$ m and $L_{abs}=L_g=2$ m in India.

The results of the ACH obtained in this study are quite consistent with those previously. "The optimum inclination angle is 50° for a latitude of 35°. The best inclined angle for maximum ventilation is 60° in Baghdad, at latitude 33.3°. The optimum angle of inclination was also 45° at 32° latitude. This can also be seen in Figure 4.9, where a 45° angle of inclination gives quite similar results to a 60°. This is also true of the results obtained in this research. Furthermore, the summer value of ACH is greater than the winter value. This is because the solar radiation intensity is higher in the summer, allowing more heat to be absorbed into the airflow and therefore raising the fluid temperature. In turn, the air density at the entrance of the solar panel and the air density on the solar panel vary widely. In the summer, the higher density differential generates a higher-pressure difference between the inlets into the solar chimney, resulting in a higher ventilation rate

and ACH levels than in the winter. The results obtained in the previous studies also reflect the increase in ventilation rate, which has also shown an increase with intensity.

For education, meeting and waiting spaces, ACH has a minimum requirement of 2, but the ACH requirements for meeting, cooking, meeting, or medical premises range between 6 to 20. ACH is the minimum requirement in respect of ACH. Moreover, the minimum requirement for ACH is 2. As a result, it is noted that solar chimneys may only be used to create educational, meeting and waiting areas in workplaces and hotel lobbies with a tilting angle of between 30° and 1990° , as these solar chimneys produce ACHs exceeding minimum ventilation standards in India.

4.6 The impact of the air gap on ACH

The influence of air gap on ACH variation has been looked into from 0.15 to 0.75 m. The consequences of Figure 4.10 and 4.11 are shown by the ACH air gap in the roof and the wall-mounted solar chimney. The rise in the air gap was found as a result of the development of ACH in this investigation. With an average ACH of 16.1 for the air gap of 0.75 meters, the maximum ventilation rates for the roof-assembled solar chimney were reached for June, while the ACH rates were 3.5 for the air gap of 0.15 m, in the same month as shown in figure 4.10. The highest ACHs were found in June and July for the solar wall chimney, 13.4 m and 2.8 for both the air gap of 0.75 m and the air gap of 0.15 m, as shown in Figure 4.11 respectively for June and January. This led the ACH to increase by more than 4 times as the air divide of 0.60 m increases. The trend in this thesis is consistent with the previous thesis, which showed an increasing air ventilation rate with an increase in air gap.

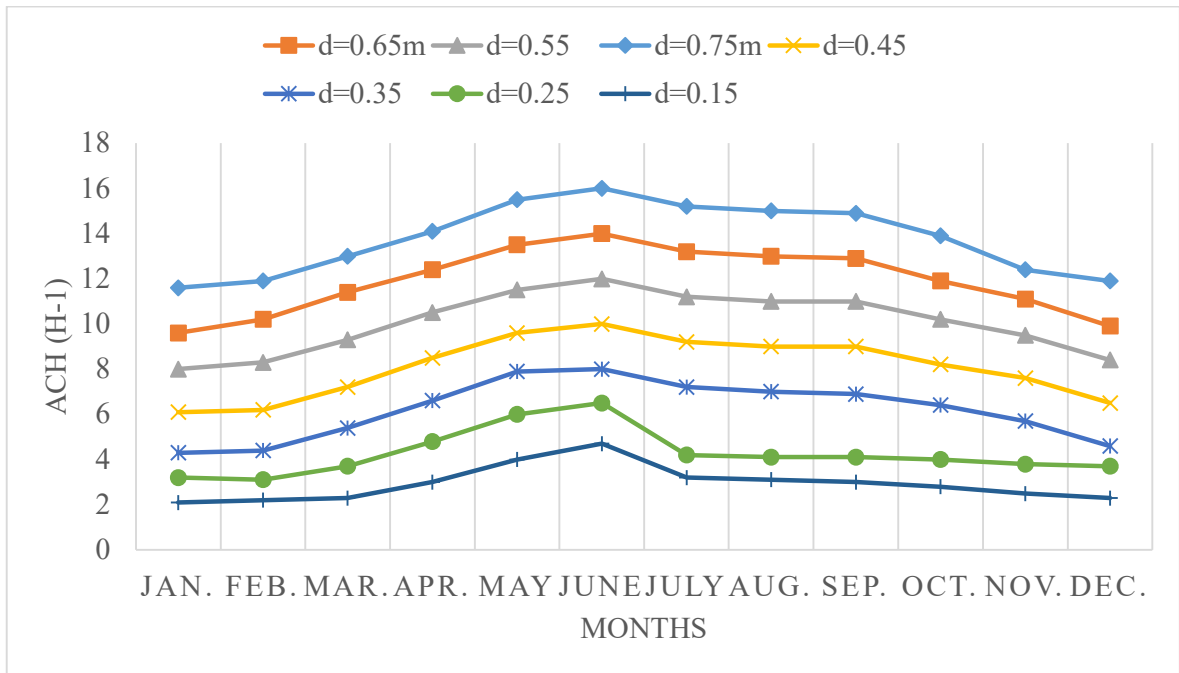


Figure 4.10: Air gap effect on average monthly hourly ACH for roof mounted solar chimney through inclined angle of 34° through Labs=Lg=2 m in India.

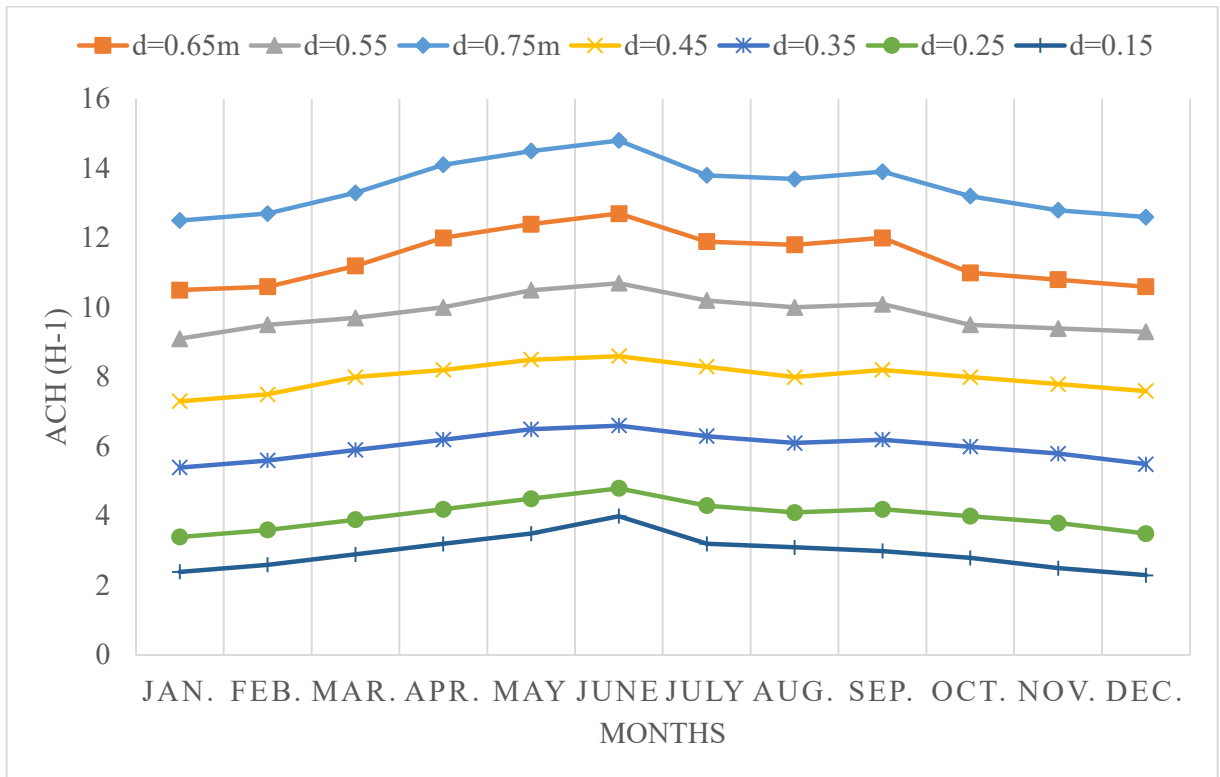


Figure 4.11: Air gap effect on average monthly ACH for wall mounted solar chimney through Labs=Lg=2 m in India.

But several previous studies have shown different results than the results of this study. The air gap increased, air velocity decreased, but it was determined that the air gap nearly had no effect on the chimney performance, since the air gap increased at the ventilation rate almost insufficiently. The ventilation rate is raised to the optimal air gap, but the air gap grows even further to lower the ventilation rate. The air divide is also growing. When the air gap is too large, reverse flow occurs in the solar chimney channel, according to the researchers. Moreover, with the increase in air gaps, the air flow has increased to an ideal air gap, but a further increase in air gaps has a negligent impact on the air flow.

4.7 Effect of chimney height on ACH

To examine the effect of the height of the chimney on the ACH, the length of the absorbent wall & glass cover was changed between 0.5 m and 3 m. The increase in the height of the chimney increases ACH for the roof and wall-mounted solar chimney, as seen

in Figures 4.12 and 4.13. It may be because, as the chimney height rises, the absorber wall's surface absorbs more solar radiation, allowing for a greater transfer of heat into the air flow through convection, resulting in increased air ventilation.

The solar on the roof with a 3m chimney height was 6.8 for June, whereas the ACH was 2.5 for a 0.5 m chimney height in the same month, as shown in Figure 4.12. In June, the ACH was 2.5. Alternatively, the value of ACH for the solar chimney wall-assembled at 3 meters & 0.5 meters of chimney, respectively, for June was 5.7 and 2.3, as can be shown in Fig. 4.13. The height of the chimney, thus, may be increased from 0.5 meter up to 3 meters to improve the rate of ventilation more than twice.

The research results are consistent with earlier research, which also showed that an enhanced rate of ventilation might be attained by increasing chimney height.

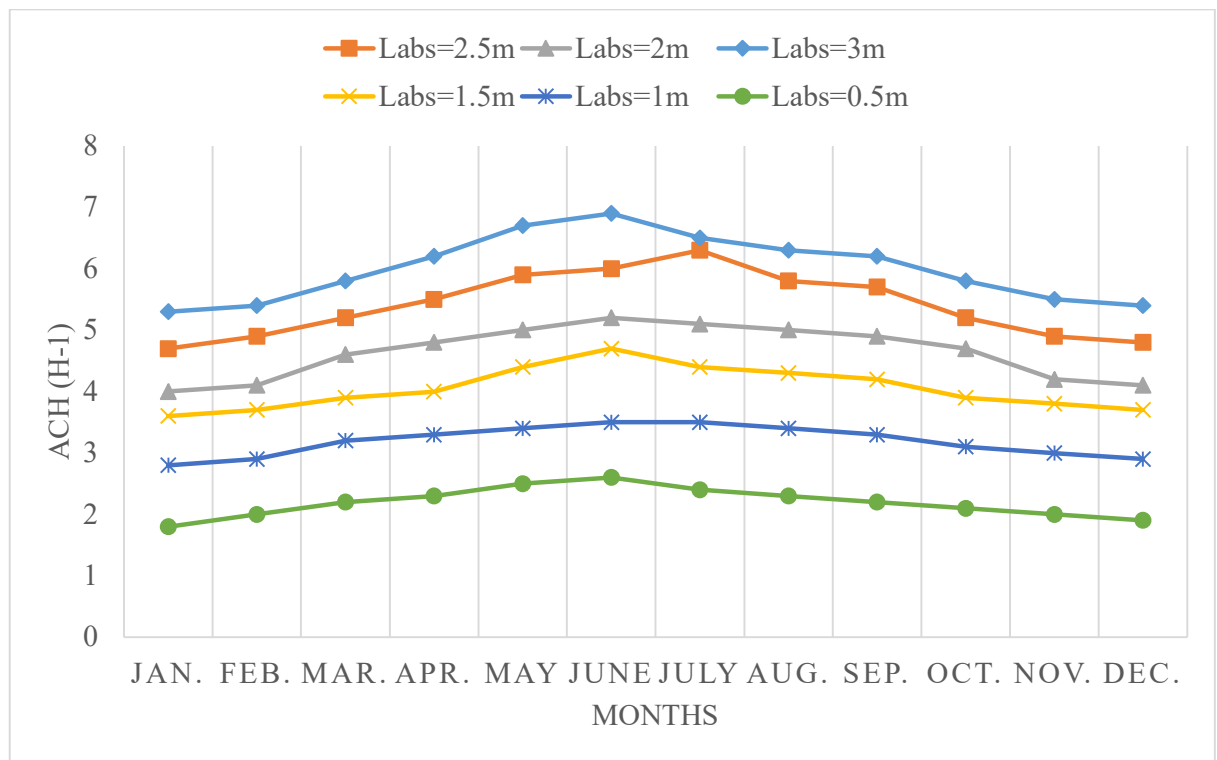


Figure 4.12: Chimney height effect on average monthly ACH for roof mounted solar chimney with inclined angle of 34° through d= 0.25 m in India.

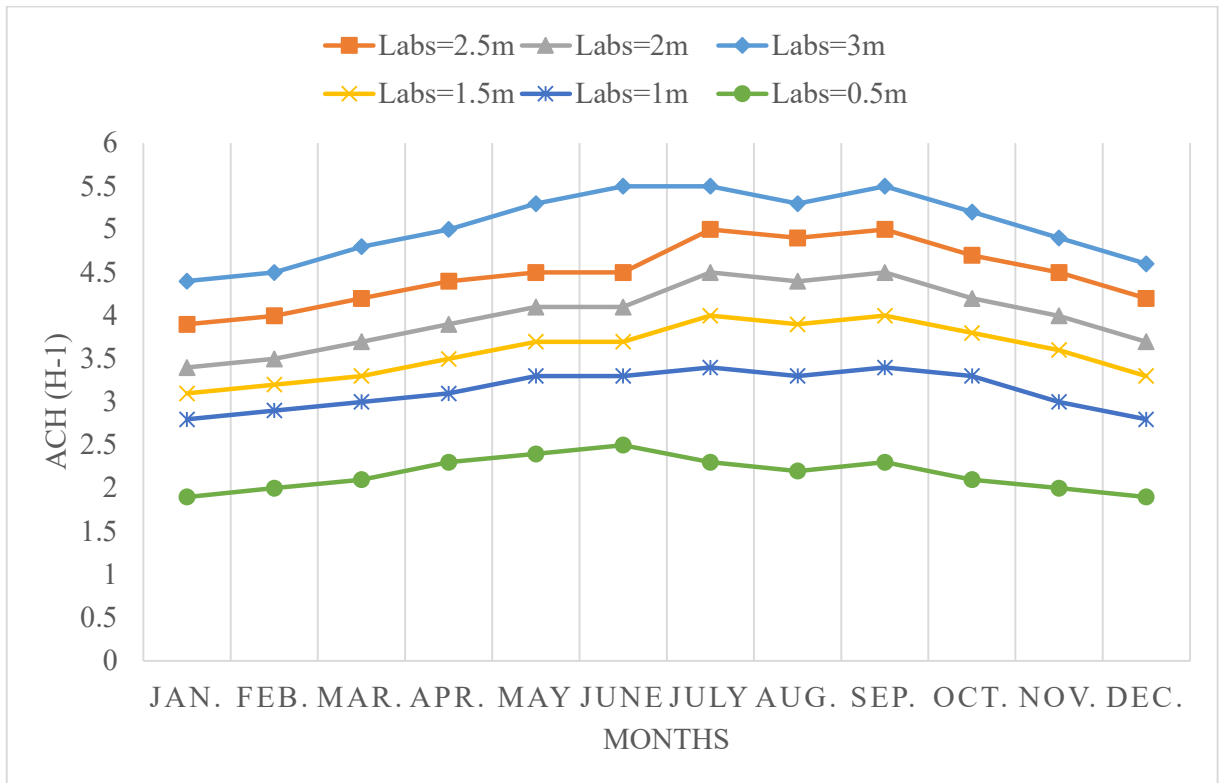


Figure 4.13: Chimney height effect on average monthly ACH for wall mounted solar chimney through $d= 0.25$ m in India.

4.8 Effect of view factor

When transferring radiative heat between two surfaces, the view factor is an important parameter. The factor of view depends on the geometry of radiative heat on both sides, thus affecting the radiative heat transfer rate between the two sides. The impact of the view factor on the radiative heat transfer coefficient between the glass cover & absorber wall, as well as the absorber's wall temperature and ACH, was investigated in this study.

4.8.1 The influence of the view factor on the radiative heat transfer coefficient between the absorber wall and the glass cover

When a view factor is taken into account, the radiation heat transfer coefficient from the absorber wall to the glass cover appears to be reduced, as shown in Figure 4.14. It could be due to the fact that, when taking into consideration the view factor, a feasible radiation value is obtained from the absorber wall of the glass cover; hence, the radiative

heat transfer coefficient from the wall into the glass is lower because the amount of radiation from the absorber wall cannot be overestimated. When the coefficient of heat transfer of $6.4 \text{ W/m}^2\text{-K}$ was ignored during June, the view factor was considered at $4.8 \text{ W/m}^2\text{-K}$. The view factor is considered. In contrast, the figure for the heat transfer radiation coefficient during July was $5.3 \text{ W/m}^2\text{-K}$ for the vertical solar chimney without a view factor, and $3.9 \text{ W/m}^2\text{-K}$ with the view factor. When the view factor was considered, the heat transfer coefficient between the absorber wall and the glass cover was found to be nearly 30% lower.

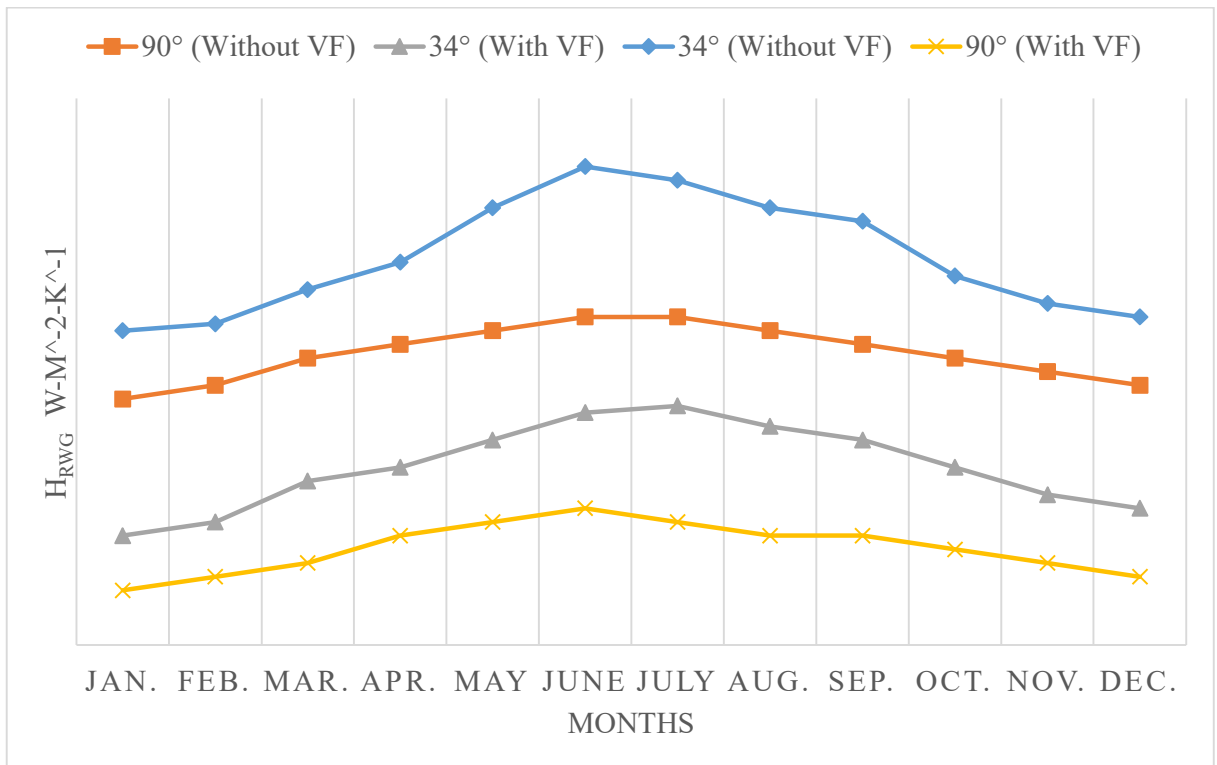


Figure 4.14: View Factor effect on average monthly coefficient of radiative heat transfer from absorber wall to the glass cover (h_{rwg}) for roof & wall mounted solar chimney through $d=0.25 \text{ m}$ and $L_{abs}=L_g=2 \text{ m}$ in India.

4.8.2 View factor going on absorber wall temperatures

At the wall absorber temperature, the impact of the sun chimney panorama factor with a 34° inclined angle and the vertical solar chimney may be shown in Figure 4.17. When the view factor is taken into account, it can be seen that the absorber wall

temperatures are higher. This may be done because if the view factor is not included, the intensity of radiation from the absorption wall to the glass coat is overstated. The percentage of radiation remaining on the absorber wall, leading to reduced temperature measurements, is therefore generally undervalued.

In June, the absorber wall temperature in the solar chimney was 58.6°C, although it was considered to be only 54.3 °C without the view factor. The vertical solar chimney, on the other hand, recorded a temperature of 30.8 °C in June whenever the view factor was taken into account, but only 29.8 °C when the view factor was not taken into account. The temperature of the inclined solar chimney's wall-absorber was consequently about 9% higher, while the view factor of the vertical solar chimney was just 3% higher. The effect of the view factor therefore influences the temperature of the absorber wall of the sloping solar chimney considerably more than the vertical solar chimneys. The solar radiation obtained on the vertical chimney absorber wall is much lower than on the solar-inclined chimney, resulting in a lesser impact on the vertical temperature of the solar-chimney-wall absorber.

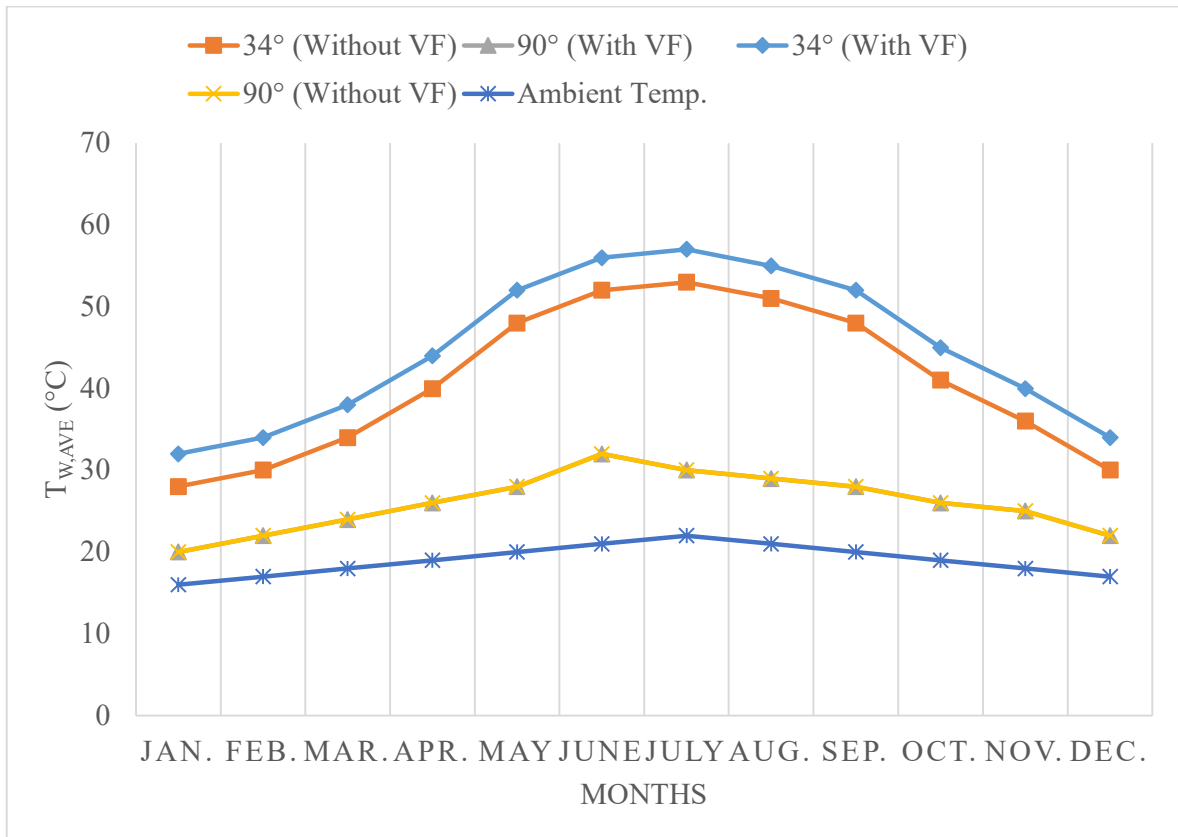


Figure 4.15: View Factor effect on average monthly absorber wall temperature for roof and wall mounted solar chimney; with $d=0.25$ m and $L_{abs}=L_g=2$ m in India.

4.8.3 View factor effect on ACH

When the view factor is taken into account for both inclined and vertical solar chimneys, the ACH is slightly greater, as illustrated in Figure 4.16. In June, when the view factor and the ACH 5.4 were assessed, the inclined solar chimney was produced, but the view factor was not taken into account. ACH 4.7 with view factor was achieved in June with a vertical solar chimney, while an ACH value of 4.5 without view factor was achieved. It is therefore possible to conclude that the ACH is 4% greater if the visibility factor is taken into consideration in both vertical and sloping solar chimneys. This may be explained by the possibility of transferring more heat into the airflow when taking into account the view factors, thus increasing the fluid temperature, resulting in a higher density difference

and thus more air being discharged from the solar chimney. As a result, if the view factor is appropriately regarded, the ventilation rate is higher.

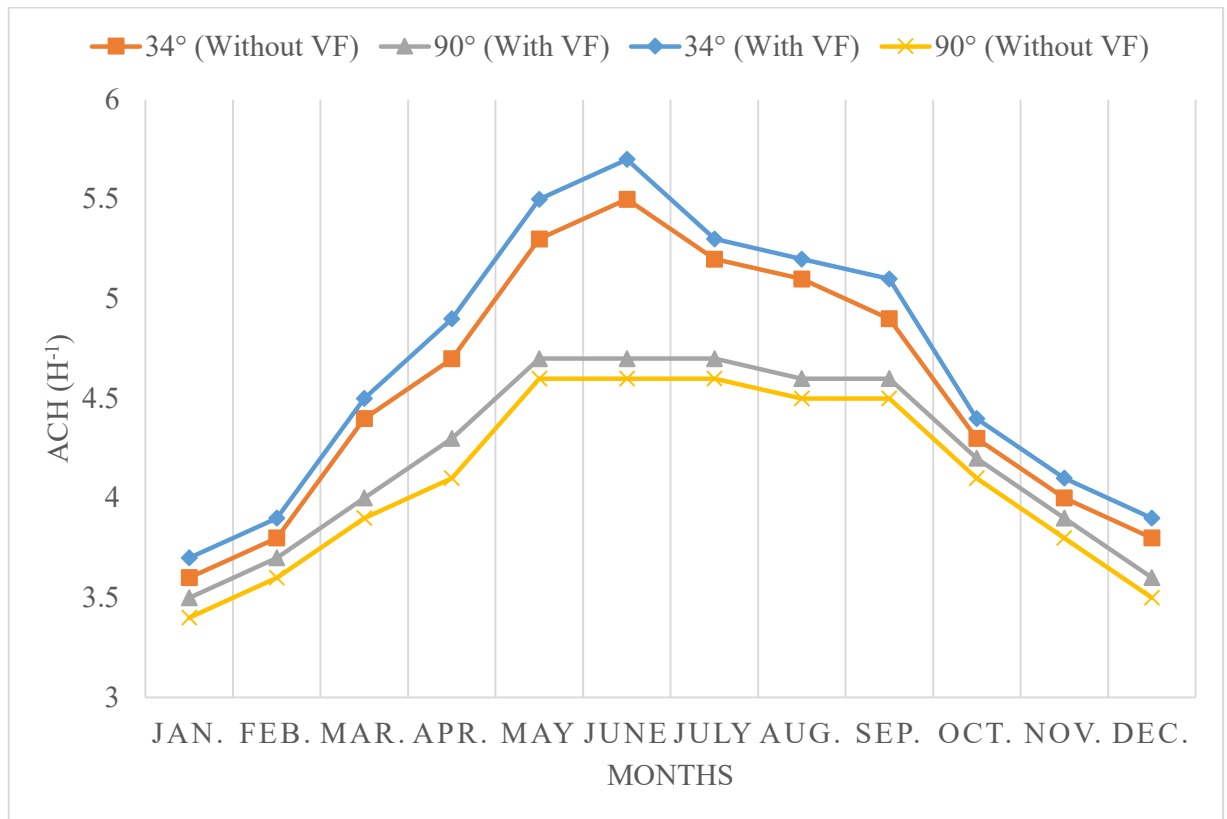


Figure 4.16: View factor effect on average monthly ACH for roof & wall mounted solar chimney; through $d=0.25$ m and $L_{abs}=L_g=2$ m in India.

4.8.4 View factor effect on ACH for various air gap values

For various levels of air gap, the view factor's effect on ACH has also been examined. When taking into consideration the view factor and ignoring the view factor to assess the influence of different ACH gap values on the view factor, ACH graphs from various air gap values have been created. The effect of the ACH view factor is displayed in Figures 4.17 and 4.18 for different air gap values of the roof and wall solar chimney. As the air space rises, the resulting effect of the view factor becomes increasingly important, as the distance between the curves increases with the air gap. In June, there was a solar chimney with an ACH-mounted roof value of 16.8 with a gap of 0.75m, and only 16.1 without a single air gap. But ACH reached a gap of 0.15 m in the same month at a view

factor of 3.6, which was identical to a gap of 0.15 m without a view factor as shown in Figure 4.15. In June, the wall-mounted solar chimney achieved an ACH of 14.7 with a 0.75-meter air gap and a view factor, compared to 13.4 without the view factor. An air gap of 0.15 meters was reached by an ACH of 2.9 during this month when both the view factor and the view factor were taken into consideration.

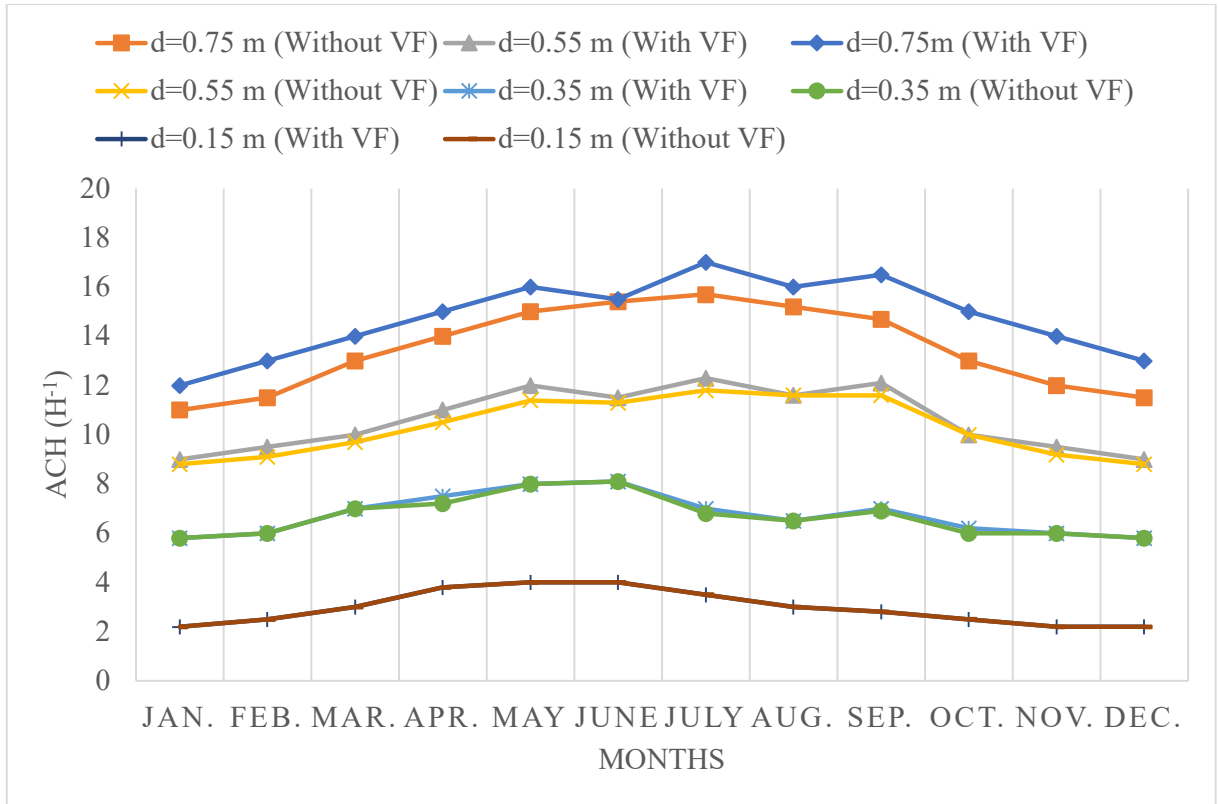


Figure 4.17: View Factor (VF) effect on average monthly ACH for variable air gaps for roof mounted solar chimney with inclined angle of 34° and Labs=Lg=2 m in India.

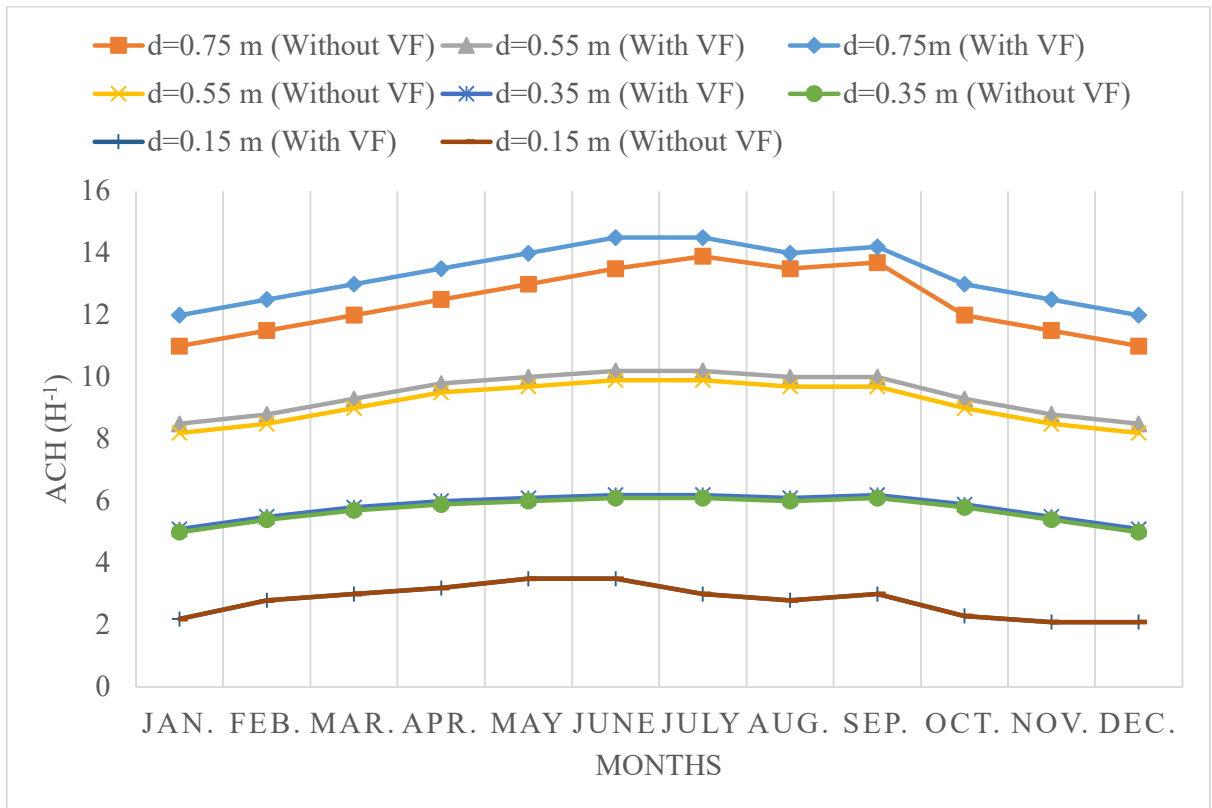


Figure 4.18: View factor effect on average monthly ACH for variable air gaps for wall mounted solar chimney with Labs=Lg=2 m in India.

4.8.5 Changes in chimney height have an effect on ACH

Figures 4.19 and 4.20 indicate how the view factor affects the ACH at various chimney heights. The ACH values can be observed slightly higher when taking account of the view factor for the solar chimneys on the roof and on the wall. The roof mounted solar chimney with a chimney height of 3 meter was attained in June with a view factor of ACH 7.1, whereas the view factor was not included in the chimney in Figure 4.19 with a view of just 6.8 meter in the same month. But in June an ACH of 5.8 was attained with a chimney height of 3 m for vertical solar chimneys, if an ACH of 5.7 was acquired, after ACH had been adjusted as seen in Fig. 4.20.

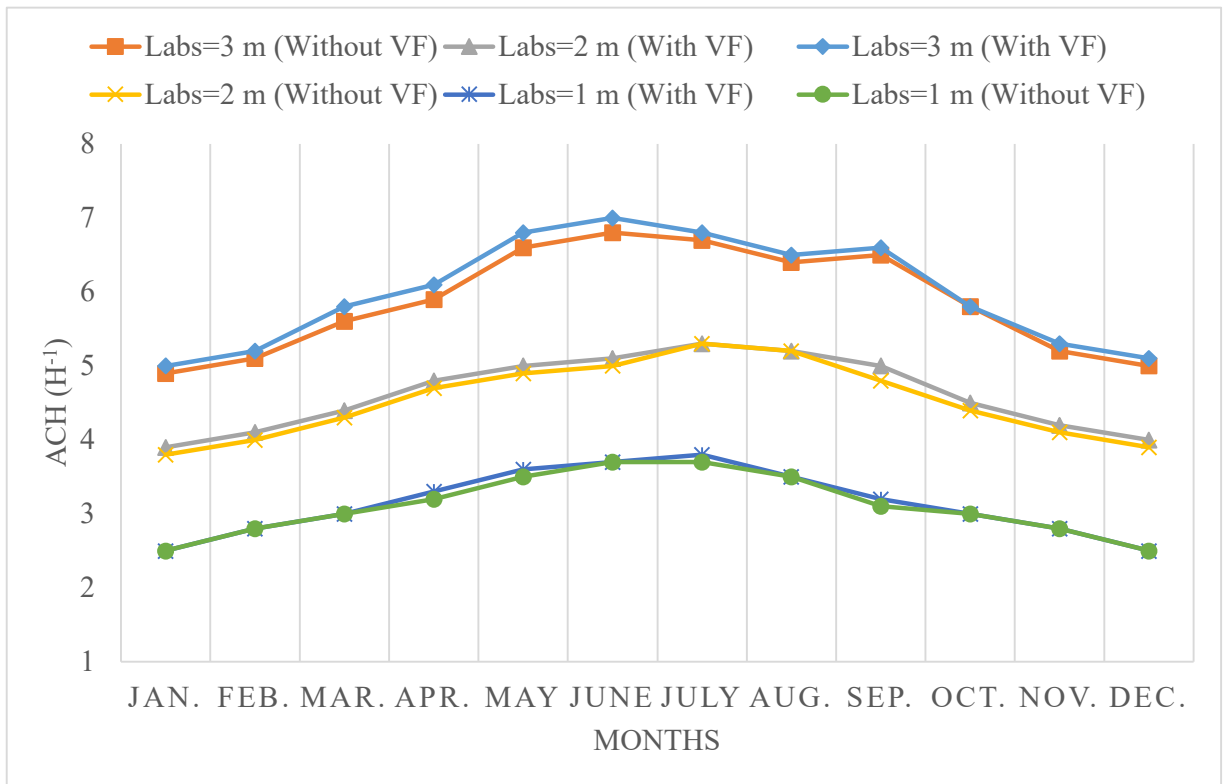


Figure 4.19: View factor effect on average monthly ACH for variable heights of chimney for roof mounted solar chimney with incline angle of 34° and d=0.25 m in India.

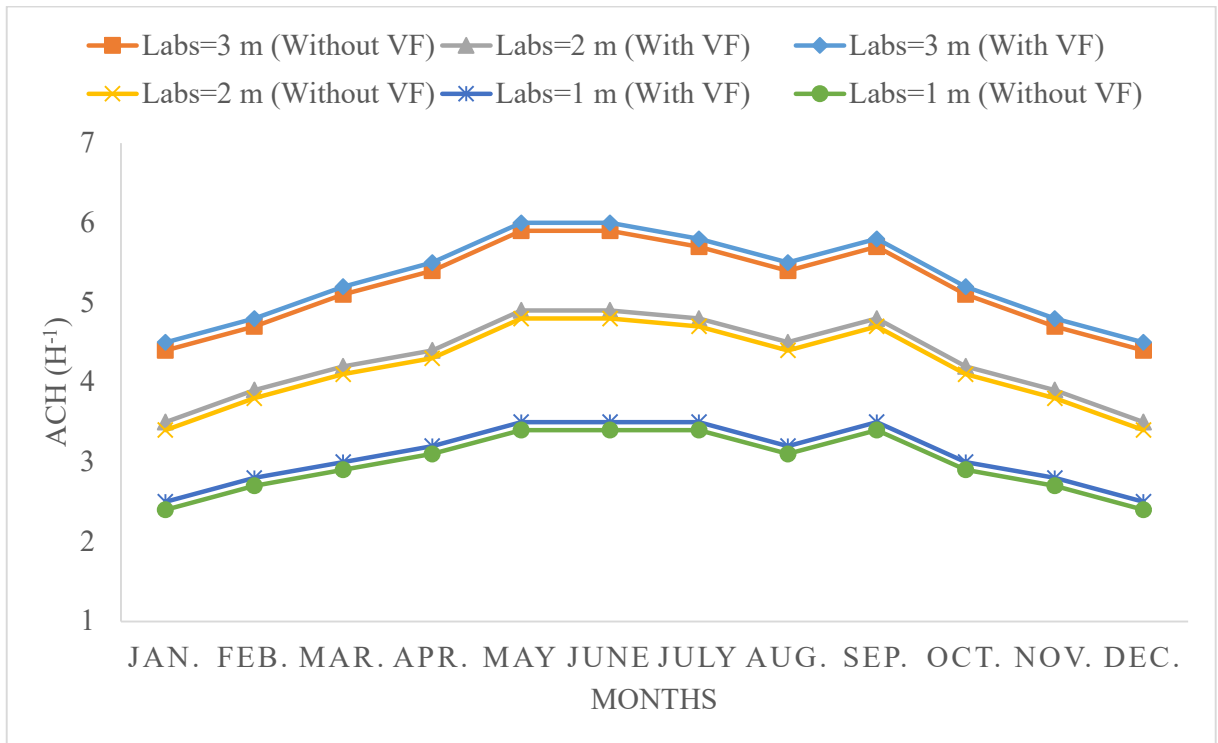


Figure 4.20: View factor effect on average monthly ACH for variable heights of chimney for wall mounted solar chimney through $d=0.25$ m in India.

Moreover, the space between the curves from 4.19 and 4.20 rises considerably as the height of the chimney increases. Also, the view factor would be seen. The ACH-curve with the view factor at 1 m is quite similar to the ACH-curve without the view factor. However, as the height of the chimney rises, so does the distance between the curves, increasing the impact of the view factor.

CHAPTER 5

5. CONCLUSION & RECOMMENDATION

Chapter 1 discusses the application of natural ventilation research in buildings during the last few years. A solar chimney can successfully reduce electricity consumption associated with mechanical ventilation in buildings while also reducing the use of fossil fuels to help control rising temperatures. The objective of this research was to compare the thermal efficiency of vertical wall-mounted and inclined solar chimneys on the roof. The following objectives were defined in order to achieve this goal:

- Develop solar chimneys that are vertical and sloped.
- Develop a solar chimney mathematical model based on a fundamental understanding of the solar chimney.
- Simulate solar chimney thermal performance, and
- Establish which solar chimney configuration is more efficient.

Chapter 4 showed and discussed numerically the results of the CFD simulation. The conclusions and recommendations are examined in this current chapter.

5.1 Conclusions

The angle of this study group ranged from 30 to 90 degrees and the air gap was around 0.15 to 0.75 meters and the height of the chimney was around 0.5 m to 3 m. Furthermore, as indicated in Chapter 4, the design element of a solar chimney has been mostly addressed, and this study is also aimed at studying the effect of the view factor on the solar chimney's thermal performance. The following observations were drawn based on the data and discussions in Chapter 4:

5.1.1 Mathematical Model Validation

The numerical results of this study and the experimental values based on the literature were in agreement. It is 13 percent view factor & 20 percent without display factor were found for inclined solar chimney models. Thus, valid and thorough modelling

of solar chimneys with the addition of view factor may be employed to stimulate the mathematical models created in the study.

5.1.2 Optimal solar chimney inclination angle

At 60° inclination, the solar chimney provided a consistently high amount of air variation per hour (ACH) throughout the year, with the least amount of ACH produced by the vertical Solar Chimney over the whole year. Therefore, it is determined that, when the tilt angles are 60° in the Northern Hemisphere, the optimum heat efficiency of a solar chimney may be achieved at a latitude of 34°.

5.1.3 Solar chimney Optimum air gap

A maximum ACH with an air gap of 0.75m was found during this study. It was observed that the ACH increased as the air space for the roof & wall mounted solar chimney increased. It is the conclusion that the larger air gap in a solar chimney offers better performance than those with smaller air gaps in solar chimneys.

5.1.4 Optimal height of Solar Chimney

A 3-meter-high chimney might reach the maximum ACH. The height of the chimney was raised, which improved the ACH. A solar chimney of 3 m in height may be further obtained to achieve a higher performance than that of a lesser height.

5.1.5 The main functional view factor in solar chimney design

CFD simulation results showed that higher wall absorber temperatures may be reached with the view factor of both the angled solar chimney and the vertical solar chimney. Furthermore, when the view factor was considered, the ACH values were found to be higher. The effects of the view factor were also more visible for large air gaps and chimney heights. Therefore, the view factor is a key element for the design of both tilted and vertically solar chimneys. If the view element isn't taken into account, the result is likely to be overestimated. In addition, it is possible to finish with an absorption of the view factor to achieve almost seven percent solar chimney mathematical modelling, which is based on model validation.

5.2 Recommendations

In this survey, a solar roof chimney performed better than a wall-mounted solar chimney. Furthermore, a tilt angle of 60° was found to be the best tilt angle for a solar chimney. Furthermore, it was determined that the view factor is a critical element in the construction of a solar chimney as its inclusion would result in an accurate ACH value. In addition, solar chimneys have been proven to produce higher air ventilation rates with huge air gaps and chimney height. However, further study is needed, and there are prospective studies that might be executed below.

5.2.1 Construction of physical models of solar chimneys placed on roof and wall-mounted

Because this investigation is limited in time, prototypes of the solar chimneys could not be constructed to evaluate their performance using experimental observations. For experimentation and comparison of experimental values with those obtained from research, prototypes of solar chimneys on the walls and roof are essential.

5.2.2 Make a comparison with other sites' results

This study could apply a mathematical model to other sites across India to see if roof-assembled solar chimneys do better than sloping solar chimneys at such sites. In addition, this model can also be employed by changing geographical parameters in the simulation of solar chimneys throughout the world.

5.2.3 Investigate the model and the effects of additional factors on solar chimney performance

This study might use the mathematical model to explore the influence of additional parameters which have not been taken into consideration in this investigation. The thermal impact of solar chimneys on the kind of glazing, the type of isolation and the thickness of the insulating material, for example, may be studied.

5.2.4 Carry out an economic analysis on the feasibility

A cost estimate for integrating a solar chimney into a building could be determined by conducting a feasibility study. A real-life scenario could be followed by the

mathematical model produced in this investigation. It could be calculated that the energy consumed was reduced by integrating a solar chimney into the building. In addition, the influence of the glass type chosen on system expenses may be studied.

CHAPTER 6

6. REFERENCE

- [1] N. K. Bansal, R. Mathur, and M. S. Bhandari, "Solar chimney for enhanced stack ventilation," *Building and Environment*, vol. 28, no. 3, pp. 373–377, 1993, doi: 10.1016/0360-1323(93)90042-2.
- [2] R. Bassiouny and N. S. A. Koura, "An analytical and numerical study of solar chimney use for room natural ventilation," *Energy and Buildings*, vol. 40, no. 5, pp. 865–873, 2008, doi: 10.1016/j.enbuild.2007.06.005.
- [3] J. Marti, M. H.-C.-S. Energy, and undefined 2007, "Dynamic physical model for a solar chimney," *Elsevier*, Accessed: Jul. 23, 2021. [Online]. Available: https://sci-hub.do/https://www.sciencedirect.com/science/article/pii/S0038092X06002222?casa_token=SNF9ztua3bwAAAAA:PABDYGb8BA_EP5i1kUKSe5Zj2a-NrEhI8YNX_iPiQb8wcRxUNwyRMLFeubyC-g2LmzeyLqjN5nY
- [4] S. Chungloo, B. L.-B. and Environment, and undefined 2007, "Application of passive cooling systems in the hot and humid climate: The case study of solar chimney and wetted roof in Thailand," *Elsevier*, Accessed: Jul. 23, 2021. [Online]. Available: https://sci-hub.do/https://www.sciencedirect.com/science/article/pii/S036013230600254X?casa_token=3MIUwMg-lEMAAAAA:VIDgEVclZbvgrD-q7oPIJ2Pzbhjp_SHLdvN4xp_-jImW7jiq1EWpJ0OMGLQUwoGwR1nHVOpNw
- [5] S. Burek, A. H.-E. and Buildings, and undefined 2007, "Air flow and thermal efficiency characteristics in solar chimneys and Trombe Walls," *Elsevier*, Accessed: Aug. 01, 2021. [Online]. Available: https://sci-hub.do/https://www.sciencedirect.com/science/article/pii/S0378778806001356?casa_token=leG4AuvissUAAAAA:XIJ-4FiLMB_GR9xZm_eeiUkFlrTqh_3z4-MXAU5zPuof0Nlio471mc8xIy8MeHCRlz43UtUZwVE
- [6] J. Mathur, S. M.-E. and Buildings, and undefined 2006, "Summer-performance of inclined roof solar chimney for natural ventilation," *Elsevier*, Accessed: Aug. 01, 2021. [Online]. Available: https://sci-hub.do/https://www.sciencedirect.com/science/article/pii/S0378778806000375?casa_token

n=j4w6MGioPv8AAAAA:RILrph3GHIQh4OPBenOnX4PsB-
EZ2Fsv32lxr2fIijKsOqg43FsPQBvyZynjshgSTCQMjyEwvik

- [7] N. Khan, Y. Su, and S. B. Riffat, "A review on wind driven ventilation techniques," *Energy and Buildings*, vol. 40, no. 8, pp. 1586–1604, 2008, doi: 10.1016/j.enbuild.2008.02.015.
- [8] M. Gontikaki, Dipl.-I. M. J. L. M. Trcka, I. Hensen, and P.-J. Hoes, "Optimization of a solar chimney design to enhance natural ventilation in a multi-storey office building."
- [9] S. L. Reinman, "Intergovernmental Panel on Climate Change (IPCC)201280 Intergovernmental Panel on Climate Change (IPCC). Geneva: World Meteorological Organization and United Nations Environment Programme Last visited October 2011. Gratis URL: www.ipcc.ch/," *Reference Reviews*, vol. 26, no. 2, pp. 41–42, Feb. 2012, doi: 10.1108/09504121211205250/FULL/HTML.
- [10] user, "NUMERICAL STUDY OF THE THERMAL PERFORMANCE OF SOLAR CHIMNEYS FOR VENTILATION IN BUILDINGS," 2015.
- [11] Z. Chen, P. Bandopadhyay, ... J. H.-B. and, and undefined 2003, "An experimental investigation of a solar chimney model with uniform wall heat flux," *Elsevier*, Accessed: Jul. 31, 2021. [Online]. Available: https://scihub.do/https://www.sciencedirect.com/science/article/pii/S036013230300057X?casa_token=_wGnQ9THo6cAAAAA:K7xbhlQz9UA4SVa5jzipH-x5x37tPx80JCXT4Dmu2gH2n9koZ3b271Y17IRcpU0To6NgJU5OrcE
- [12] D. Charitar, "Numerical study of the thermal performance of solar chimneys for ventilation in buildings," 2015, Accessed: Jul. 31, 2021. [Online]. Available: <https://scihub.do/https://open.uct.ac.za/handle/11427/20100>
- [13] J. Hirunlabh, W. Kongduang, P. Namprakai, J. K.-R. Energy, and undefined 1999, "Study of natural ventilation of houses by a metallic solar wall under tropical climate," *Elsevier*, Accessed: Jul. 31, 2021. [Online]. Available: https://scihub.do/https://www.sciencedirect.com/science/article/pii/S0960148198007836?casa_token=gIcxU38BQ_AAAAAA:CQP5QxHLGUiCGlkmLd0cXk_oHNACMqa4gG1NVWocnhcIcysGCM_7q_FJiST1JNi9gW6OPVnzQUw

- [14] C. Afonso and A. Oliveira, "Solar chimneys: Simulation and experiment," *Energy and Buildings*, vol. 32, no. 1, pp. 71–79, 2000, doi: 10.1016/S0378-7788(99)00038-9.
- [15] M. Maerefat, A. H.-R. Energy, and undefined 2010, "Passive cooling of buildings by using integrated earth to air heat exchanger and solar chimney," *Elsevier*, Accessed: Jul. 31, 2021. [Online]. Available: https://sci-hub.do/https://www.sciencedirect.com/science/article/pii/S0960148110001059?casa_token=w8miWYLFtFQAAAAA:h5VgCo0pYW1NAC4xTK-R_pnNE4z8w25x8oUxPT22D9A1DB66sFOa7aIuZ6m1MglOVpBpUb91OgQ
- [16] Z. Chen, P. Bandopadhyay, ... J. H.-B. and, and undefined 2003, "An experimental investigation of a solar chimney model with uniform wall heat flux," *Elsevier*, Accessed: Jul. 31, 2021. [Online]. Available: https://sci-hub.do/https://www.sciencedirect.com/science/article/pii/S036013230300057X?casa_token=VAJ8mc-u4GQAAAAA:Az7fbF458fKoMaayTpvvwE-wMnapyoyUfhfj-rUr4j1bPsHgRhRRmhsZS4WVsrNifQtEDbmamGw
- [17] D. Harris, N. H.-A. Energy, and undefined 2007, "Solar chimney and building ventilation," *Elsevier*, Accessed: Jul. 31, 2021. [Online]. Available: https://sci-hub.do/https://www.sciencedirect.com/science/article/pii/S0306261906000808?casa_token=XoSgMTJcNO4AAAAA:EAJwkiFtSMzZD38WDc42-gT2WZnv2eZ9hNb7kLVsnxbZQbe-0Jy64m4RqqSpbvUSyxLsfUGUkRI
- [18] D. Charitar, "Numerical study of the thermal performance of solar chimneys for ventilation in buildings," 2015, Accessed: Jul. 31, 2021. [Online]. Available: <https://sci-hub.do/https://open.uct.ac.za/handle/11427/20100>
- [19] A. Imran, J. Jalil, S. A.-R. Energy, and undefined 2015, "Induced flow for ventilation and cooling by a solar chimney," *Elsevier*, Accessed: Jul. 31, 2021. [Online]. Available: https://sci-hub.do/https://www.sciencedirect.com/science/article/pii/S0960148115000269?casa_token=CUVDHhPqXhFqMAAAAA:Pn9lhxtkEXV5CxJ4U4NGsVU0VzeWE-YkLaOnT1niQ2oPZdHCijZ4Ltlac0t9Jy669KdHXScmfA
- [20] X. Jianliu, L. W.-E. and Buildings, and undefined 2013, "Study on solar chimney used for room natural ventilation in Nanjing," *Elsevier*, Accessed: Jul. 31, 2021. [Online].

- Available: https://sci-hub.do/https://www.sciencedirect.com/science/article/pii/S0378778813004246?casa_token=X4SM5F5U8DgAAAAA:Z1x-1Mdqeyi7Q_Il5cq3uKQ610ZA7FJWoeGs1G8ZpLOF7oPR_v3lFmoWDabU1rnlTDyv2V5_zx4
- [21] G. Gan, S. R.-A. T. Engineering, and undefined 1998, “A numerical study of solar chimney for natural ventilation of buildings with heat recovery,” *Elsevier*, Accessed: Jul. 31, 2021. [Online]. Available: https://sci-hub.do/https://www.sciencedirect.com/science/article/pii/S1359431197001178?casa_token=Q2k2uf5HBG8AAAAA:HrxXRS_fIIEsF4T79V0PXHky6_3ahCDjUWvvu0Ct0P0Pwr7WCLmKkFg2gXqZQxbwdRXIospjdhg
- [22] D. Harris, N. H.-A. Energy, and undefined 2007, “Solar chimney and building ventilation,” *Elsevier*, Accessed: Jul. 31, 2021. [Online]. Available: https://sci-hub.do/https://www.sciencedirect.com/science/article/pii/S0306261906000808?casa_token=o7f-KFkx3I0AAAAA:SaKzSXayTADiRRqc88_Ka1aVm3I7svU__Rbcll6bD8gF2DyNEbh_4p4LJInX36hiKh7XV530FPc
- [23] R. Khanal, C. L.-E. and Buildings, and undefined 2011, “Solar chimney—A passive strategy for natural ventilation,” *Elsevier*, Accessed: Jul. 31, 2021. [Online]. Available: https://sci-hub.do/https://www.sciencedirect.com/science/article/pii/S0378778811001447?casa_token=pNv-KmBtsBcAAAAA:Agjw8GywCS5sULE3wV81uxxJGdplKfrDlkqIETWJkC54_NxRMX9Rj66qnOBIBkLfBu-H7iZ6PrU
- [24] N. Bansal, R. Mathur, M. B.-B. and environment, and undefined 1993, “Solar chimney for enhanced stack ventilation,” *Elsevier*, Accessed: Jul. 31, 2021. [Online]. Available: <https://sci-hub.do/https://www.sciencedirect.com/science/article/pii/0360132393900422>
- [25] J. Hirunlabh, W. Kongduang, P. Namprakai, J. K.-R. Energy, and undefined 1999, “Study of natural ventilation of houses by a metallic solar wall under tropical climate,” *Elsevier*, Accessed: Jul. 31, 2021. [Online]. Available: <https://sci-hub.do/https://www.sciencedirect.com/science/article/pii/S0378778899000422>

hub.do/https://www.sciencedirect.com/science/article/pii/S0960148198007836?casa_token=_ERmag18Vw0AAAAA:S-dBCRL3sUobyjMnxJWS4XT05VNM3QIbxda9GHccGjhN9AxDOMb-NUW4j3YyCDuE4xhQhsYH3FE

- [26] J. Mathur, N. Bansal, S. Mathur, M. J.-S. Energy, and undefined 2006, "Experimental investigations on solar chimney for room ventilation," *Elsevier*, Accessed: Jul. 31, 2021. [Online]. Available: https://sci-hub.do/https://www.sciencedirect.com/science/article/pii/S0038092X05003014?casa_token=n6_cSaTwdswAAAAA:9UnStOMs0Xajo2p8CsHB5d2I9Wp1eY-u4n4w_G2YBIJY82ACtMMglBoPtTSHNBwdFo5qq22UX40
- [27] K. Ong, C. C.-S. energy, and undefined 2003, "Performance of a solar chimney," *Elsevier*, Accessed: Jul. 31, 2021. [Online]. Available: https://sci-hub.do/https://www.sciencedirect.com/science/article/pii/S0038092X03001142?casa_token=EH4PoFSZ-5AAAAAA:GxeECrf-ej8qJMuW6DAaeGWZFiotdzyM4b1_BFd2KNXTy4oJVI5jsdF_79FVYn7he3opTbjTjho
- [28] T. Miyazaki, A. Akisawa, T. K.-R. Energy, and undefined 2006, "The effects of solar chimneys on thermal load mitigation of office buildings under the Japanese climate," *Elsevier*, Accessed: Jul. 31, 2021. [Online]. Available: https://sci-hub.do/https://www.sciencedirect.com/science/article/pii/S0960148105001175?casa_token=teSlZOEWqK0AAAAA:m1TdZuOzKEGKpFDPTSHvz-PmeZXGxa8qNo5jO96wJtVVzEdMSyHciPDVS9tyJVLGUiP8IOw8I3k
- [29] A. Imran, J. Jalil, S. A.-R. Energy, and undefined 2015, "Induced flow for ventilation and cooling by a solar chimney," *Elsevier*, Accessed: Jul. 31, 2021. [Online]. Available: https://sci-hub.do/https://www.sciencedirect.com/science/article/pii/S0960148115000269?casa_token=2nDGftDF14gAAAAA:AvbsddbMvJYpmwKpNLYAeMr3FunLbmdJjWPsWP4VsaM41nSwqC_esTFxPYQT1PbeWU5bpRqHslA